Superconductivity

CHAPTER OUTLINE

14.1 PROPERTIES OF SUPERCONDUCTORS

14.1.1 Introduction

The main source of electrical resistance in a metal is the electron–phonon interaction caused by the scattering of the electrons due to vibrations of the ions. This is the lattice excitations in bulk metals, which corresponds to small ionic vibrations ($d/L \ll 1$), where d is the amplitude of the vibrations and L is the lattice period. This is described as acoustic quanta (phonons) with energies,

$$\varepsilon_{ph}^i = \hbar\Omega_i(\mathbf{q}),$$ (14.1)

where $\mathbf{q} = \hbar\mathbf{k}$ is the momentum of the phonon, and $|\mathbf{k}| = 2\pi/\lambda$, where λ is the phonon's wavelength. Here, i corresponds to the various phonon branches (longitudinal, transverse, and optical). The electron–lattice interaction, i.e., the energy exchange between the electrons and lattice, is due to the radiation and adsorption of phonons and is known as the electron–phonon interaction. As the temperature is lowered, the amplitude of the ions becomes smaller, and the electrical resistance is reduced.

But the resistivity of a normal metal does not become zero at zero temperature because there are other sources of electrical resistance due to the presence of impurities and imperfections in the crystal structure. As the temperature is reduced, there is a residual resistivity ρ_0 at absolute zero that is approximately 1% of the resistivity of a pure sample. The temperature around which the resistivity is constant is approximately $1°$ K. The resistivity of a metal can be expressed as

$$\rho(T) = \rho_0 + AT^5,$$ (14.2)

where ρ_0 is the residual resistivity, and AT^5 is the term arising from electron–phonon scattering. The variation of resistivity with temperature for a non-superconducting metal is shown in Figure 14.1.

The phenomenon of superconductivity was discovered by Kammerlingh Onnes in 1911.[15] He measured the resistivity of platinum and found that the resistivity followed a curve similar to the curve shown in Figure 14.1. However, when he performed a similar experiment with a sample of mercury, he found that the resistance of the sample dropped sharply to a value of zero at $4.2°$ K. The metals of which the resistivity becomes zero at a particular temperature are known as superconductors. The temperature at

FIGURE 14.1

Variation of resistivity of a normal metal.

or below which a metal becomes a superconductor is called the critical temperature, T_c. Thus, there are two types of metals: some that become superconductors at or below T_c and others that continue to have resistivity even at 0° K. The variation of resistivity with temperature for a superconducting metal is shown in Figure 14.2.

14.1.2 Type I and Type II Superconductors

The experimental results displayed in the previous section were for metals when there was no external magnetic field. However, when an external magnetic field H is applied, the superconducting state is destroyed above a critical

FIGURE 14.2

Variation of resistivity with temperature of a superconducting metal.

external magnetic field H_c. This type of a superconductor is called a type I superconductor. From experiment results, one can obtain a relationship between the critical magnetic field H_T, which destroys superconductivity at a given temperature T,

$$H_T = H_c \left[1 - \left(\frac{T}{T_c} \right)^2 \right]. \tag{14.3}$$

This experimental result is plotted in Figure 14.3.

One can distinguish type I and type II superconductors in the following manner. In type I superconductors, the diamagnetism grows linearly with the magnetic field until the critical value is reached. This is shown in Figure 14.4.
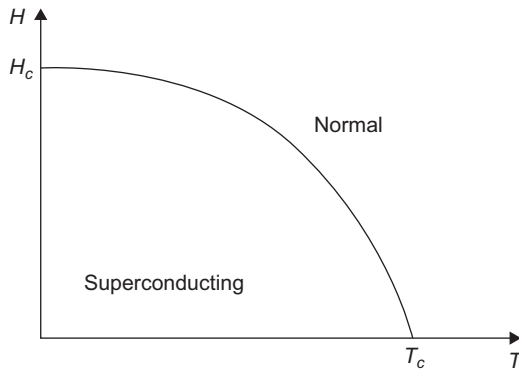

FIGURE 14.3

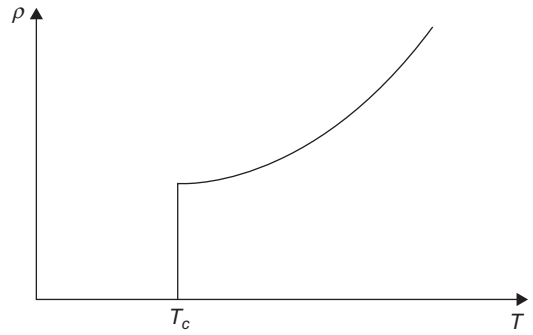Variation of external magnetic field H against temperature T in a type I superconductor.
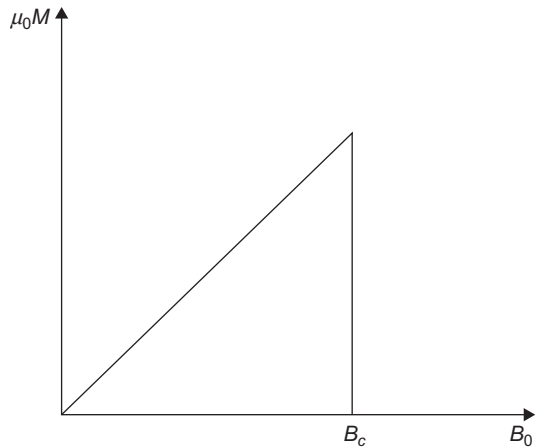

FIGURE 14.4

Type I superconductor.

In type II superconductors, the diamagnetization is linear with the external field up to a value B_{c1}, but the magnetization decreases when the flux begins to penetrate the metal. This is shown in Figure 14.5.

14.1.3 Second-Order Phase Transition

The transition from the normal (N) state to the superconducting (S) state is known as a second-order phase transition. In the first-order phase transitions, the heat capacity is continuous, whereas in second-order phase transitions, the heat capacity is discontinuous. Figure 14.6 schematically shows the variation of heat capacity from a normal state to a superconducting state.

14.1.4 Isotope Effect

It was discovered in 1950 that the different isotopes of the same element possess different transition temperatures to enter the superconducting state,

$$T_c M_i^\alpha = \text{constant}, \qquad (14.4)$$

where M_i is the isotopic mass of the same element. Usually, $\alpha \approx 1/2$. This was a strong indication that the interaction of the electrons with ions in the lattice was important for superconductivity.

14.1.5 Phase Diagram

Superconductivity is destroyed by application of a large magnetic field. In addition, superconductivity is destroyed if the current exceeds a "critical current." This is known as the Silsbee effect. To summarize, superconductivity depends on three factors: (a) the temperature T, (b) the external magnetic field H, and (c) the current density j. This type of dependence on three different experimental parameters is shown as a three-dimensional curve in Figure 14.7.
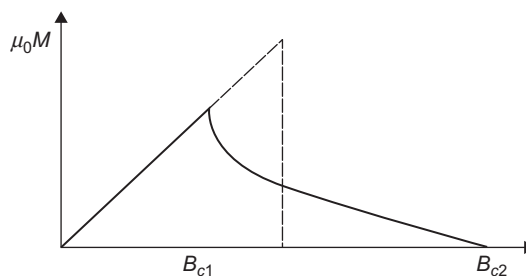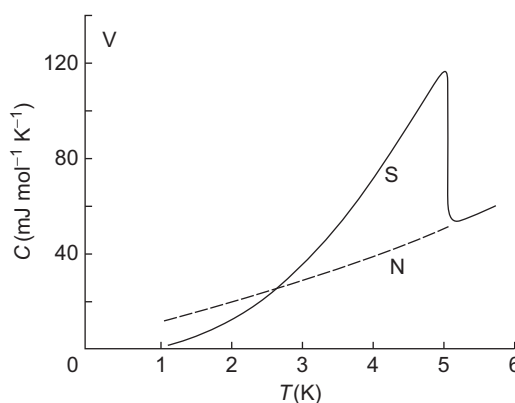

FIGURE 14.5

Type II superconductor.

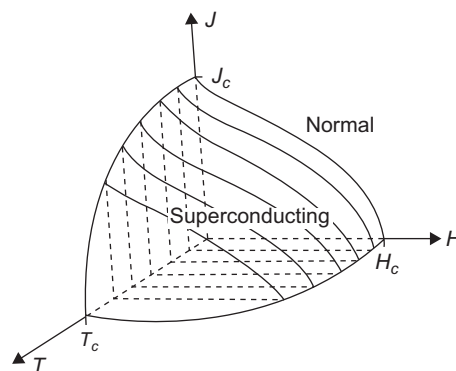**FIGURE 14.6**

Second-order phase transition.

FIGURE 14.7

Critical surface separating the superconducting and normal states.

14.2 MEISSNER–OCHSENFELD EFFECT

Meissner and Ochsenfeld observed that an external magnetic field (as long as it is not too large) cannot penetrate inside a superconductor.[22] Thus, a superconductor behaves as a perfect diamagnet. If a normal metal is cooled below the critical temperature in a magnetic field, the magnetic flux is expelled abruptly. The transition to the superconducting state in a magnetic field is accompanied by the surface currents necessary to cancel the magnetic field inside the specimen. This scenario is shown in Figure 14.8.
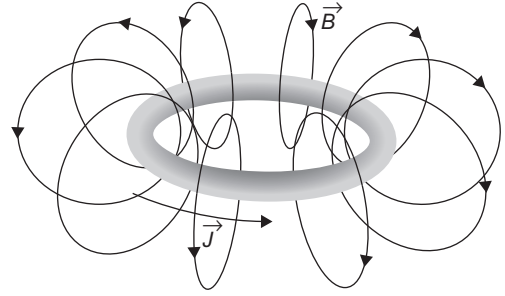
FIGURE 14.8

Flux lines cannot pass through the current loop in a superconductor.

14.3 THE LONDON EQUATION

London and London explained the Meissner–Ochsenfeld effect by adopting the two-fluid model of Gorter and Casimir.[18] The basic assumption of their model is that there are two types of electrons, $n_s(T)$ (density of superconducting electrons) and n (density of total number of conducting electrons), in a metal in the superconducting state. At temperatures $T < T_c$, only a fraction $n_s(T)/n$ of the total number of conduction electrons can carry a supercurrent. $n_s(T) \to 0$ as $T \to T_c \cdot n - n_s$ cannot carry an electric current without dissipation. In a small electric field, the normal electrons that flow parallel to the superconducting electrons are inert and therefore ignored while discussing the motion of electrons. In the presence of an electric field $\mathbf{E}$,

$$m\dot{\mathbf{v}}_s = -e\mathbf{E}, \tag{14.5}$$

where $\mathbf{v}_s$ is the mean velocity of superconducting electrons. Because the current density $\mathbf{j} = -e\mathbf{v}_s n_s$, Eq. (14.5) can be rewritten in the alternate form

$$\frac{d\mathbf{j}}{dt} = \frac{n_s e^2}{m}\mathbf{E}. \tag{14.6}$$

From Eq. (14.6) and Faraday's law of induction,

$$\overrightarrow{\nabla} \times \mathrm{E} = -\frac{1}{c}\frac{\partial \mathbf{B}}{\partial t}, \tag{14.7}$$

we obtain

$$\frac{\partial}{\partial t}\left(\overrightarrow{\nabla} \times \mathrm{j} + \frac{n_s e^2}{mc}\mathbf{B}\right) = 0. \tag{14.8}$$

It is easy to show that Maxwell's equation (neglecting the displacement current $\mathbf{D}$ as well as replacing $\mathbf{H}$ with $\mathbf{B}$ because $\mathbf{j}$ is the mean microscopic current) can be written as (Problem 14.1)

$$\overrightarrow{\nabla} \times \mathrm{B} = \frac{4\pi}{c}\mathbf{j}. \tag{14.9}$$

Because Eqs. (14.8) and (14.9) are consistent with any static magnetic field and the Meissner–Ochsenfeld (Ref. 22) effect requires that the magnetic field be expelled in the superconducting state, London and London (Ref. 18) postulated that

$$\left(\overrightarrow{\nabla} \times j + \frac{n_s e^2}{mc}\mathbf{B}\right) = 0. \tag{14.10}$$

Using the vector identity,

$$\overrightarrow{\nabla} \times (\overrightarrow{\nabla} \times V) = \overrightarrow{\nabla}(\overrightarrow{\nabla} \cdot \mathbf{V}) - \nabla^2 \mathbf{V}, \tag{14.11}$$

we obtain from Eqs. (14.9) through (14.11),

$$\nabla^2 \mathbf{B} = \frac{4\pi n_s e^2}{mc^2}\mathbf{B} \tag{14.12}$$

and

$$\nabla^2 \mathbf{j} = \frac{4\pi n_s e^2}{mc^2}\mathbf{j}. \tag{14.13}$$

Eqs. (14.12) and (14.13) predict that the magnetic fields and currents in a superconductor can exist within a layer of thickness λ_L, known as the London penetration depth,

$$\lambda_L = \left(\frac{mc^2}{4\pi n_s e^2}\right)^{\frac{1}{2}}. \tag{14.14}$$

One can rewrite λ_L in the alternate form

$$\lambda_L = 41.9\left(\frac{r_s}{a_0}\right)^{3/2}\left(\frac{n}{n_s}\right)^{1/2}\overset{\circ}{\text{A}}. \tag{14.15}$$

Thus, when $T << T_c$, $(n \approx n_s)$ the surface currents that screen out the applied magnetic field occur within a layer of $10^2 - 10^3$ Å. The magnetic field drops continuously to zero within this layer. It has indeed been observed experimentally that the field penetration is incomplete in superconducting films that are thinner than λ_L.

14.4 GINZBURG–LANDAU THEORY
14.4.1 Order Parameter

Landau and Ginzburg[17] described the superconductivity state through a position-dependent order parameter $\Psi(\mathbf{r}) = |\Psi(\mathbf{r})|e^{i\phi(\mathbf{r})}$, which describes the macroscopic properties of a superfluid condensate.[17] The superfluid density $n_s(\mathbf{r}) = |\Psi(\mathbf{r})|^2$, suggesting that $\Psi(\mathbf{r})$ is a wave function that vanishes at T_c. Landau and Ginzburg (Ref. 17) guessed that to be able to study the magnetic and thermodynamic properties of superconductors, the total free energy F_s with respect to its value in the normal state F_n should be

$$F_s = F_n + \int d\mathbf{r}\left[\alpha|\Psi|^2 + \frac{\beta}{2}|\Psi|^4 + \frac{1}{8\pi}B^2 + \frac{1}{2m^*}\left|\left[\frac{\hbar}{i}\overrightarrow{\nabla} + \frac{e^*}{c}\mathbf{A}(\mathbf{r})\right]\Psi(\mathbf{r})\right|^2\right]. \tag{14.16}$$

Here, the first two terms are from Landau's general theory of second-order phase transition borrowed from their theory for liquid ^{4}He. According to their phenomenological model, one assumes that the complete ground-state wave function $\psi_N(\mathbf{r}_1......\mathbf{r}_N)$ for N electrons is known. If an extra electron is added, one knows $\psi_{N+1}(\mathbf{r}_1......\mathbf{r}_{N+1})$. We define

$$\Psi(\mathbf{r}) = \int d^N\mathbf{r}\psi_N^*(\mathbf{r}_1......\mathbf{r}_N)\psi_{N+1}(\mathbf{r}_1......\mathbf{r}_N, \mathbf{r}). \tag{14.17}$$

Far away from $\mathbf{r}$, Ψ_N and Ψ_{N+1} coincide, but in its neighborhood Ψ_{N+1} accommodates one extra particle. The last two terms are due to the fact that the superconducting electron wave function might interact with the vector potential like a single macroscopic particle of effective charge e^* (it was later found that $e^* = 2e$, *consistent with Cooper pairs* (Ref. 7)). Minimizing Eq. (14.16) with respect to $\mathbf{A}$, we obtain

$$\overrightarrow{\nabla} \times \mathbf{B} = \frac{4\pi}{c}\mathbf{j}, \tag{14.18}$$

where

$$\mathbf{j}(\mathbf{r}) = \frac{-e^*\hbar}{2im^*}\left[\Psi^*\overrightarrow{\nabla}\Psi - \Psi\overrightarrow{\nabla}\Psi^*\right] - \frac{e^{*2}}{m^*c}\mathbf{A}\Psi^*\Psi. \tag{14.19}$$

Minimizing Eq. (14.16) with respect to Ψ^*, by first integrating such that all spatial derivatives act on Ψ and then taking functional derivatives with respect to Ψ^*, we obtain (Problem 14.3)

$$\left[\alpha + \beta|\Psi|^2 + \frac{1}{2m^*}\left(\frac{\hbar}{i}\overrightarrow{\nabla} + \frac{e^*}{c}\mathbf{A}\right)^2\right]\Psi = 0. \tag{14.20}$$

Eqs. (14.19) and (14.20) are known as the Landau–Ginzburg (Ref. 17) equations.

14.4.2 Boundary Conditions

No current can flow out of the boundary when a superconductor is in contact with a vacuum. Thus, one can write

$$\hat{n} \cdot \left(\frac{\hbar}{i}\overrightarrow{\nabla} + \frac{e^*}{c}\mathbf{A}\right) = 0. \tag{14.21}$$

The additional boundary condition imposed by Landau and Ginzburg[17] is that $\Psi = 0$ was not considered as an acceptable condition, because in that case, it would be impossible to obtain solutions for thin superconducting films.

14.4.3 Coherence Length

The coherence length ξ specifies the scale for variation of the order parameter Ψ. The coherence length is defined by

$$\xi = \left[\frac{\hbar^2}{2m^*|\alpha|}\right]^{\frac{1}{2}}, \tag{14.22}$$

where α is defined in Eq. (14.20). If the external magnetic field vanishes, Eq. (14.20) can be rewritten as

$$|\Psi|^2 = \Psi_0^2 = -\frac{\alpha}{\beta} \text{ or } |\Psi|^2 = 0. \tag{14.23}$$

Because β is positive (otherwise, F is minimized when $\Psi \to \infty$), $\alpha < 0$, which corresponds to a uniform superconducting state. The free energy per unit volume is given by Eq. (14.16),

$$F_s - F_N = -\frac{\alpha^2}{2\beta}. \tag{14.24}$$

It can be easily shown that

$$\Delta F = F_N - F_s = \frac{H_c^2}{8\pi}. \tag{14.25}$$

From Eqs. (14.24) and (14.25), we obtain

$$H_c^2 = \frac{4\pi\alpha^2}{\beta}. \tag{14.26}$$

We can scale the order parameter for superconductors,

$$\psi = \frac{\Psi}{\Psi_0}. \tag{14.27}$$

From Eqs. (14.20), (14.22), and (14.27), we obtain for $\mathbf{A} = 0$,

$$-\xi^2 \nabla^2 \psi - \psi + \psi|\psi|^2 = 0. \tag{14.28}$$

Thus, the coherence length ξ is the characteristic scale on which ψ varies (in the absence of a magnetic field).

14.4.4 London Penetration Depth

In Eq. (14.19), in the presence of a weak magnetic field, $\Psi \approx \Psi_0$ for $x < 0$. Thus, we obtain from Eqs. (14.18) and (14.19),

$$\mathbf{j} = \frac{c}{4\pi} \overrightarrow{\nabla} \times \mathbf{B} = -\frac{e^{*2}}{m^*c} \Psi_0^2 \mathbf{A} \tag{14.29}$$

and

$$\nabla \times \nabla \times \mathbf{B} = -\frac{4\pi}{c} \frac{e^{*2}}{m^*c} \Psi_0^2 \mathbf{B} = -\frac{\mathbf{B}}{\lambda_L^2}. \tag{14.30}$$

Because $m^* = 2m$, $e^* = 2e$, and $\Psi_0^2 = -\frac{\alpha}{\beta}$, λ_L is the London penetration depth defined in Eq. (14.14). The parameter

$$\kappa = \lambda_L/\xi = \frac{m^*c}{e\hbar} \sqrt{\frac{\beta}{2\pi}} \tag{14.31}$$

is the only parameter in Landau–Ginzburg theory.

It can be easily shown that the surface energy is positive if $\kappa < 1/\sqrt{2}$ and negative if $\kappa > 1/\sqrt{2}$. The magnetic flux can easily penetrate a superconductor if the surface energy is negative and can form type II superconductors, which are interlocking regions of normal and superconducting metal. Type I superconductors are those for which $\kappa < 1/\sqrt{2}$ and the flux cannot penetrate.

Consider a magnetic field $H > H_c$ so that $\Psi = 0$ because superconductivity is destroyed. When the field is gradually lowered, considering only the first-order terms in Ψ (because $\mathbf{j} = 0$),

$$\left[\alpha + \frac{1}{2m^*}\left(\frac{\hbar}{i}\overrightarrow{\nabla} + \frac{e^*}{c}\mathbf{A}\right)^2\right]\Psi = 0. \tag{14.32}$$

Eq. (14.32) is an eigenvalue equation of a charge ($e^* = 2e$) in a constant magnetic field, the lowest energy is $\hbar\omega_c/2$, and because H_{c2} is the largest magnetic field that permits a solution,

$$\omega_c = \frac{e^* H_{c2}}{m^* c}. \tag{14.33}$$

From Eqs. (14.32) and (14.33),

$$-\alpha\Psi = \frac{\hbar e^* H_{c2}}{2m^* c}\Psi \tag{14.34}$$

or

$$|\alpha| = \frac{\hbar e H_{c2}}{m^* c}. \tag{14.35}$$

From Eqs. (14.26), (14.31), and (14.35), we obtain

$$\frac{H_{c2}}{H_c} = \sqrt{2}\kappa. \tag{14.36}$$

14.5 **FLUX QUANTIZATION**

In Eq. (14.18), if we substitute

$$\Psi(\mathbf{r}) = \Psi_0 e^{i\phi(\mathbf{r})}, \tag{14.37}$$

where $\phi(\mathbf{r})$ is real, we obtain from Eqs. (14.18) and (14.37)

$$\mathbf{j} = -\frac{\Psi_0^2}{m^*}\left(\frac{e^{*2}}{c}\mathbf{A} + e^*\hbar\overrightarrow{\nabla}\phi\right), \tag{14.38}$$

which can be rewritten in the alternate form

$$\overrightarrow{\nabla}\phi = -\frac{1}{\hbar}\left(\frac{m^*}{e^*\Psi_0^2}\mathbf{j} + \frac{e^*}{c}\mathbf{A}\right). \tag{14.39}$$

If we consider a superconductor in the shape of a ring (Figure 14.9), which shows a path encircling the aperture but lying well within the interior,

$$\oint \mathbf{j} \cdot d\mathbf{l} = 0. \tag{14.40}$$
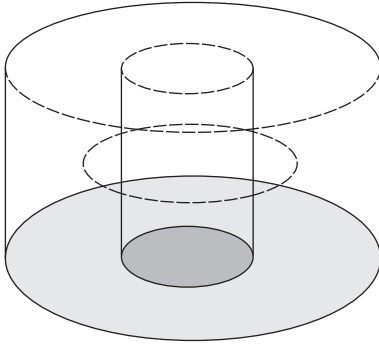
FIGURE 14.9

A path encircling the aperture ring of
superconducting material.

From Eqs. (14.23) and (14.24), we obtain

$$\oint \overrightarrow{\nabla} \phi \cdot d\mathbf{l} = -\oint \frac{e^*\mathbf{A}}{\hbar c} \cdot d\mathbf{l}. \tag{14.41}$$

From Stoke's theorem,

$$\oint \mathbf{A} \cdot d\mathbf{l} = \oint \overrightarrow{\nabla} \times \mathbf{A} \cdot d\mathbf{S} = \oint \mathbf{B} \cdot d\mathbf{S} = \Phi, \tag{14.42}$$

where Φ is the flux enclosed by the ring. We note
that because the magnetic field cannot penetrate a
superconducting material, the enclosed flux is inde-
pendent of the choice of the path. In addition, the
order parameter Ψ is single-valued, and hence, its
phase changes by $2\pi n$ (n is an integer) when the
ring is encircled. Thus, we have

$$\oint \overrightarrow{\nabla} \phi \cdot d\mathbf{l} = 2\pi n. \tag{14.43}$$

From Eqs. (14.41) through (14.43), we obtain

$$\frac{-e^*}{\hbar c}\Phi = 2\pi n. \tag{14.44}$$

Defining a fluxoid or a flux quantum,

$$\Phi_0 \equiv \frac{hc}{2e} = 2.0679 \text{ G cm}^2, \tag{14.45}$$

we obtain from Eqs. (14.43) and (14.44)

$$|\Phi| = \frac{2ne}{e^*}\Phi_0. \tag{14.46}$$

The integrated magnetic flux that penetrates a hole through a superconductor is quantized in units of
$(2e/e^*)\Phi_0$. Thus, $e^* = 2e$, confirming the fact that the microscopic theory of superconductivity
involves pairing of electrons. Flux quantization was experimentally observed independently by
Deaver and Fairbank[8] and Doll and Nabauer.[12]

14.6 JOSEPHSON EFFECT
14.6.1 Two Superconductors Separated by an Oxide Layer
In 1962, Josephson (Refs. 13, 14) predicted that if two superconductors were separated by a small
strip of nonsuperconducting material (shown in Figure 14.10), the wave function would oscillate
because it would interfere with itself. The two superconductors would interact through their small
residues while decaying through the barrier. Due to tunneling, the change in energy $\Delta\varepsilon$ is given by

$$\Delta\varepsilon = \int d\mathbf{r} f(\mathbf{r})\left(\Psi_1^*(\mathbf{r})\Psi_2(\mathbf{r}) + \Psi_1(\mathbf{r})\Psi_2^*(\mathbf{r})\right). \tag{14.47}$$
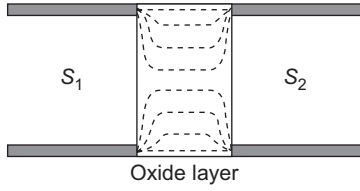
FIGURE 14.10

The oxide layer between two superconductors S_1 and S_2.

At some reference point in the bulk, if the macroscopic wave functions are Ψ_1 and Ψ_2,

$$\Delta\varepsilon = \in(\Psi_1^*\Psi_2 + \Psi_1\Psi_2^*), \qquad (14.48)$$

where $\in$ is a very small quantity. The Schrodinger equations for Ψ_1 and Ψ_2 can be written as

$$i\hbar\frac{\partial\Psi_1}{\partial t} = \varepsilon_1\Psi_1 + \in\Psi_2 \qquad (14.49)$$

and

$$i\hbar\frac{\partial\Psi_2}{\partial t} = \in\Psi_1 + \varepsilon_2\Psi_2. \qquad (14.50)$$

The wave functions are taken of the form

$$\Psi_j = \sqrt{n_j}e^{i\phi_j}, \qquad (14.51)$$

where n_j ($j = 1$ or 2) are the superconducting electron densities $n = \sqrt{n_1 n_2}$ and $n_1 \approx n_2$. Substituting Eq. (14.51) in Eqs. (14.49) and (14.50), we obtain

$$i\hbar\left(\frac{\dot{n}_1}{\sqrt{n_1}} + i\sqrt{n_1}\dot{\phi}_1\right)e^{i\phi_1} = (\varepsilon_1\sqrt{n_1}e^{i\phi_1} + \in\sqrt{n_2}e^{i\phi_2}) \qquad (14.52)$$

and

$$i\hbar\left(\frac{\dot{n}_2}{\sqrt{n_2}} + i\sqrt{n_2}\dot{\phi}_2\right)e^{i\phi_2} = (\varepsilon_2\sqrt{n_2}e^{i\phi_2} + \in\sqrt{n_1}e^{i\phi_1}). \qquad (14.53)$$

It can be easily shown from Eqs. (14.52) and (14.53) that

$$\dot{n}_1 = 2\frac{\in n}{\hbar}\sin(\phi_2 - \phi_1) = -\dot{n}_2 = \frac{j}{e^*} \qquad (14.54)$$

and

$$\dot{\phi}_2 - \dot{\phi}_1 = \frac{1}{\hbar}(\varepsilon_1 - \varepsilon_2) = \frac{e^*}{\hbar}(V_2 - V_1). \qquad (14.55)$$

We note that the phase of a wave function changes when there is a magnetic field. To make a wave function phase gauge-invariant, we have to add the line integral $\frac{e^*}{\hbar c}\int_0 d\mathbf{l}\cdot\mathbf{A}$, taken from some arbitrary reference point, to the phase. Incorporating this and taking into account the fact that $e^* = 2e$, we obtain

$$\mathbf{j} = \mathbf{j}_0\sin\left(\phi_2 - \phi_1 + \frac{2e}{\hbar c}\int_1^2 d\mathbf{l}\cdot\mathbf{A}\right) \qquad (14.56)$$

and

$$-\frac{1}{\hbar}(\varepsilon_2 - \varepsilon_1) = \frac{2eV}{\hbar} = \frac{\partial}{\partial t}\left(\phi_2 - \phi_1 + \frac{2e}{\hbar c}\int_1^2 d\mathbf{l}\cdot\mathbf{A}\right).$$

(14.57)

Here, the energy difference $\varepsilon_2 - \varepsilon_1$ is the difference in energies of electron pairs, and V is the difference of the voltage between the two superconductors.
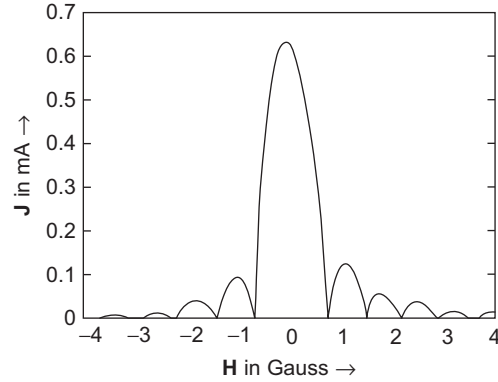

FIGURE 14.11

Maximum zero-voltage current in an Sn-SnO-Sn junction at $T = 1.9°$ K (sketch of results of R.C. Jaklevic (Ref. 23)).

14.6.2 AC and DC Josephson Effects

If we place two superconductors at different voltages in contact, then $\varepsilon_1 - \varepsilon_2 \neq 0$. Because $\phi_2 - \phi_1$ drifts in time, n_1 and n_2 oscillate about their mean values at 484 MHz/μV. This is known as the AC Josephson effect.

However, if $\varepsilon_1 - \varepsilon_2 = 0$, $\phi_1 - \phi_2$ is independent of time. Because $\phi_1 \neq \phi_2$, there is a steady current flow according to Eq. (14.56). This phenomenon is known as the DC Josephson effect. If the electrons are injected into a Josephson junction, $\phi_2 - \phi_1$ adjusts to a nonzero value. The maximum value of $\phi_2 - \phi_1$ is $\pi/2$. Thus, there is a current flow in the absence of any voltage difference (see Figure 14.11). This is a unique property of the superconductors and is a significant consequence of the Josephson effect.

14.7 MICROSCOPIC THEORY OF SUPERCONDUCTIVITY

14.7.1 Introduction

In Figure 8.14g, the graph shows an electron emitting a virtual phonon that is absorbed by a second electron. The lattice is deformed (polarized) in the vicinity of the first electron. A second electron near this polarized cloud experiences a force of repulsion or attraction that is independent of the Coulomb interaction between the two electrons. This is termed an effective electron–electron interaction via virtual phonons and is responsible for superconductivity under certain conditions. In the graph of Figure 8.14g, there are two possible intermediate states: electron $\mathbf{k}$ emits a phonon $-\mathbf{q}$, which is absorbed by electron $\mathbf{k}'$; or electron $\mathbf{k}'$ emits a phonon $\mathbf{q}$, which is absorbed by electron $\mathbf{k}$.

In Eq. (8.165), we derived an expression for electron–phonon coupling for longitudinal acoustic (LA) phonons,

$$\hat{H}_{el-ph} = \sum_{\mathbf{kq}s} M_{\mathbf{q}}(\hat{a}_{-\mathbf{q}}^\dagger + \hat{a}_{\mathbf{q}})\hat{c}_{\mathbf{k}+\mathbf{q},s}^\dagger \hat{c}_{\mathbf{k},s}.$$

(14.58)

We note that the direction of the spin is not changed by this interaction.

14.7.2 Quasi-Electrons

We now consider a system of electrons and phonons and write a Hamiltonian of the form

$$\hat{H} = \sum_{\mathbf{k},s} E(\mathbf{k})\hat{c}_{\mathbf{k}s}^{\dagger}\hat{c}_{\mathbf{k}s} + \sum_{\mathbf{q}} \hbar\omega_{\mathbf{q}}\hat{a}_{\mathbf{q}}^{\dagger}\hat{a}_{\mathbf{q}} + \sum_{\mathbf{k}\mathbf{q}} M_{\mathbf{q}}(\hat{a}_{-\mathbf{q}}^{\dagger} + \hat{a}_{\mathbf{q}})\hat{c}_{\mathbf{k}+\mathbf{q},s}^{\dagger}\hat{c}_{\mathbf{k},s} = \hat{H}_0 + \hat{H}_1, \tag{14.59}$$

where $\hat{H}_1$ is the electron–phonon interaction term. We use a canonical transformation,

$$\hat{H}_S = e^{-\hat{S}}\hat{H}e^{\hat{S}} = \hat{H}_0 + (\hat{H}_1 + [\hat{H}_0, \hat{S}]) + \frac{1}{2}[(\hat{H}_1 + [\hat{H}_0, \hat{S}], \hat{S}] + \frac{1}{2}[\hat{H}_1, \hat{S}] + \cdots. \tag{14.60}$$

If we choose $\hat{S}$ such that

$$\hat{H}_1 + [\hat{H}_0, \hat{S}] = 0, \tag{14.61}$$

the electron–phonon interaction $\hat{H}_1$ is eliminated apart from a higher-order term. We choose $\hat{S}$ of the form

$$\hat{S} = \sum_{\mathbf{k}\mathbf{q}s'} M_{\mathbf{q}}(\alpha\hat{a}_{-\mathbf{q}}^{\dagger} + \beta\hat{a}_{\mathbf{q}})\hat{c}_{\mathbf{k}+\mathbf{q},s'}^{\dagger}\hat{c}_{\mathbf{k},s'}. \tag{14.62}$$

From Eqs. (14.61) and (14.62), it can be easily shown that (Problem 14.5)

$$\alpha^{-1} = E(\mathbf{k}) - E(\mathbf{k}+\mathbf{q}) - \hbar\omega_{\mathbf{q}} \tag{14.63}$$

and

$$\beta^{-1} = E(\mathbf{k}) - E(\mathbf{k}+\mathbf{q}) + \hbar\omega_{\mathbf{q}}. \tag{14.64}$$

From Eqs. (14.60) and (14.61), the next-order interaction term is $\frac{1}{2}[\hat{H}_1, \hat{S}]$, which is a sum of terms that contain operator products of the form

$$\hat{a}_{\pm\mathbf{q}}^{\dagger}\hat{a}_{\pm\mathbf{q}'}\hat{c}_{\mathbf{k}'+\mathbf{q}',s'}^{\dagger}\hat{c}_{\mathbf{k}',s'}\hat{c}_{\mathbf{k}+\mathbf{q},s}^{\dagger}\hat{c}_{\mathbf{k},s}. \tag{14.65}$$

One can show (Problem 14.6) that because $\mathbf{q}' = -\mathbf{q}$ (from momentum conservation), only one out of all the possible combinations does not contain any phonon operators,

$$\hat{c}_{\mathbf{k}+\mathbf{q},s}^{\dagger}\hat{c}_{\mathbf{k}-\mathbf{q},s'}^{\dagger}\hat{c}_{\mathbf{k}',s'}\hat{c}_{\mathbf{k},s}, \tag{14.66}$$

when

$$\mathbf{k}' \neq \mathbf{k}, \, \mathbf{k}+\mathbf{q}. \tag{14.67}$$

From. Eqs. (14.60), (14.62), and (14.66), the explicit form for this interaction is (Problem 14.7)

$$\hat{H}_{eff} = \frac{1}{2}\sum_{\mathbf{k},\mathbf{k}',\mathbf{q},s,s'} |M_{\mathbf{q}}|^2(\alpha - \beta)\hat{c}_{\mathbf{k}+\mathbf{q},s}^{\dagger}\hat{c}_{\mathbf{k}'-\mathbf{q},s'}^{\dagger}\hat{c}_{\mathbf{k}',s'}\hat{c}_{\mathbf{k},s}. \tag{14.68}$$

Substituting the values of α and β from Eqs. (14.63) and (14.64) in Eq. (14.68), we obtain (Problem 14.8)

$$<f|\hat{H}_{eff}|i> = \frac{1}{2}\sum_{\mathbf{k},\mathbf{k}',\mathbf{q},s,s'} <f|V_{\mathbf{k}\mathbf{q}}\hat{c}_{\mathbf{k}+\mathbf{q},s}^{\dagger}\hat{c}_{\mathbf{k}-\mathbf{q},s'}^{\dagger}\hat{c}_{\mathbf{k}'s'}\hat{c}_{\mathbf{k},s}|i>, \tag{14.69}$$

where

$$V_{\mathbf{kq}} = \frac{2|M_{\mathbf{q}}|^2 \hbar\omega_{\mathbf{q}}}{[E(\mathbf{k}+\mathbf{q}) - E(\mathbf{k})]^2 - (\hbar\omega_{\mathbf{q}})^2}, \tag{14.70}$$

and $|i\rangle$ and $|f\rangle$ are the initial and final states, respectively. $V_{\mathbf{kq}}$ is essentially the Fourier coefficient of the effective interaction. When $|E(\mathbf{k}+\mathbf{q}) - E(\mathbf{k})| < \hbar\omega_{\mathbf{q}}$, $V_{\mathbf{kq}}$ is negative and the interaction is attractive, whereas the interaction is repulsive when $V_{\mathbf{kq}}$ is positive.

Omitting all the terms in the transformed Hamiltonian that contains phonon creation or annihilation operators, we obtain from Eqs. (14.59) and (14.70),

$$\hat{H}_S = \sum_{\mathbf{k}s} E(\mathbf{k}) \hat{c}_{\mathbf{k},s}^\dagger \hat{c}_{\mathbf{k},s} + \sum_{\mathbf{k},\mathbf{k}',\mathbf{q},s,s'} |M_{\mathbf{q}}|^2 \frac{\hbar\omega_{\mathbf{q}}}{[E(\mathbf{k}+\mathbf{q}) - E(\mathbf{k})]^2 - (\hbar\omega_{\mathbf{q}})^2} \hat{c}_{\mathbf{k}+\mathbf{q},s}^\dagger \hat{c}_{\mathbf{k}'-\mathbf{q},s'}^\dagger \hat{c}_{\mathbf{k}',s'} \hat{c}_{\mathbf{k},s}. \tag{14.71}$$

14.7.3 Cooper Pairs

We consider a state containing N noninteracting electron gas, which fills the Fermi sphere in $\mathbf{k}-$ space. The ground state $|G\rangle$ is the filled Fermi sphere. We introduce two electrons $\mathbf{k}_1$ and $\mathbf{k}_2$ into this system and take as the interaction between these electrons the positive part of $V_{\mathbf{kq}}$ (Eq. 14.70), which is repulsive. Thus, the interaction involving phonon exchange will take place only when $|E(\mathbf{k}+\mathbf{q}) - E(\mathbf{k})| \le \hbar\omega_{\mathbf{q}}$. The wave function of the electron pair can be written as

$$\psi_{12} = \sum_{\mathbf{k}_1 \mathbf{k}_2 s_1 s_2} A_{s_1 s_2}(\mathbf{k}_1, \mathbf{k}_2) \hat{c}_{\mathbf{k}_1 s_1}^\dagger \hat{c}_{\mathbf{k}_2 s_2}^\dagger |G\rangle. \tag{14.72}$$

The summation over $\mathbf{k}_1$ and $\mathbf{k}_2$ is carried out subject to the condition that $\mathbf{K} = \mathbf{k}_1 + \mathbf{k}_2 = $ constant in order to form a state with definite momentum. This scenario is shown in Figure 14.12.

If we consider two electrons just above the Fermi sphere, an interaction will occur only when $E(\mathbf{k}_1) \le E_F + \hbar\omega_{\mathbf{q}}$. The regions in $\mathbf{k}$ space that are summed in Eq. (14.72) are shown in the shaded areas because $\mathbf{K} = \mathbf{k}_1 + \mathbf{k}_2$. These regions are at a maximum when $\mathbf{K} = 0$.

Assuming that $\mathbf{K} = 0$, and the electron spins are antiparallel, we can rewrite Eq. (14.72) as

$$\psi_{12} = \sum_{\mathbf{k}} b(\mathbf{k}) \hat{c}_{\mathbf{k},s}^\dagger c_{-\mathbf{k},-s} |G\rangle. \tag{14.73}$$

We will explain later why only antiparallel spins are included in Eq. (14.73). We make a further approximation in Eq. (14.70) by considering $V_{\mathbf{kq}}$ to be a constant in the range of attractive interaction ($V_{\mathbf{kq}} = -U$), and $V_{\mathbf{kq}} = 0$ otherwise. In fact, from Eq. (14.71), we obtain the condition

$$U \ne 0, \text{ when } |E(\mathbf{k}+\mathbf{q}) - E(\mathbf{k})| \le \hbar\omega_{\mathbf{q}}. \tag{14.74}$$

The Debye frequency ω_D is the maximum value of $\omega_{\mathbf{q}}$ in the Debye approximation.
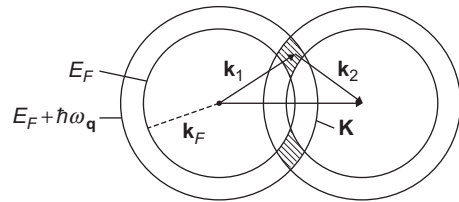

FIGURE 14.12

Here, $\mathbf{k}$ vectors of two interacting electrons ($\mathbf{K} = \mathbf{k}_1 + \mathbf{k}_2$) that lie within a shell of thickness $\hbar\omega_{\mathbf{q}}$ above E_F.

Substituting Eq. (14.74) in Eq. (14.71), we obtain

$$\hat{H} = \sum_{\mathbf{k},s} E(\mathbf{k})\hat{c}_{\mathbf{k},s}^{\dagger}\hat{c}_{\mathbf{k},s} - \frac{U}{2}\sum_{\mathbf{k},\mathbf{q},s} \hat{c}_{\mathbf{k}+\mathbf{q},s}^{\dagger}\hat{c}_{-\mathbf{k}-\mathbf{q},-s}^{\dagger}\hat{c}_{-\mathbf{k},-s}\hat{c}_{\mathbf{k},s}. \tag{14.75}$$

Here, we note that the factor ½ in the second term in Eq. (14.75) is due to the summation over only one spin index. From Eqs. (14.73) and (14.75), we obtain an expression for the energy E,

$$E = <\psi|\hat{H}|\psi> = 2\sum_{\mathbf{k}} E(\mathbf{k})|b(\mathbf{k})|^2 - U\sum_{\mathbf{k},\mathbf{q}} b^*(\mathbf{k}+\mathbf{q})b(\mathbf{k}), \tag{14.76}$$

where $b(\mathbf{k})$ is obtained by varying E subject to the condition,

$$\sum_{\mathbf{k}} |b(\mathbf{k})|^2 = 1. \tag{14.77}$$

By varying E in Eq. (14.76), we obtain

$$\frac{\partial}{\partial b_{\mathbf{k}'}^*}\left[E - \beta\sum_{\mathbf{k}'} |b(\mathbf{k}'')|^2 \right] = 2E(\mathbf{k}')b(\mathbf{k}') - U\sum_{\mathbf{q}} b(\mathbf{k}'-\mathbf{q}) - \beta b(\mathbf{k}') = 0, \tag{14.78}$$

from which we have

$$[2E(\mathbf{k}) - \beta]b(\mathbf{k}) = U\sum_{\mathbf{k}'} b(\mathbf{k}'). \tag{14.79}$$

Here, β is Lagrange's parameter and $U \neq 0$ only for the energies E_F to $E_F + \hbar\omega_{\mathbf{q}}$. One can show (Problem 14.9) that if we take the complex conjugate of Eq. (14.79), multiply by $b(\mathbf{k})$, and sum over $\mathbf{k}$, we obtain an equation that agrees with Eq. (14.76) provided $\beta = E$.

Similarly, the sum over $b(\mathbf{k}')$ is over a small number of $\mathbf{k}'$, such that we can write

$$\sum_{\mathbf{k}'} b(\mathbf{k}') = B. \tag{14.80}$$

From Eqs. (14.79) and (14.80), we obtain

$$\sum_{\mathbf{k}} b(\mathbf{k}) = B = \sum_{E(\mathbf{k})} \frac{UB}{2E(\mathbf{k}) - \beta} \tag{14.81}$$

or

$$\sum_{E(\mathbf{k})} \frac{U}{2E(\mathbf{k}) - \beta} = 1. \tag{14.82}$$

We note that if we had considered parallel spins in Eq. (14.73), the constant B would have been zero because of the antisymmetry of the spatial part of the wave function. If we take the complex conjugate of Eq. (14.79), multiply by $b(\mathbf{k})$, and sum over $\mathbf{k}$, we obtain an equation that agrees with Eq. (14.76), provided $\beta = E$ (Problem 14.9). Because $U \neq 0$ only in the range E_F and $E_F + \hbar\omega_{\mathbf{q}}$, we can rewrite Eq. (14.82) in the alternate form

$$U \int_{E_F}^{E_F+\hbar\omega_{\mathbf{q}}} \frac{D(x)dx}{2x - E} = 1, \tag{14.83}$$

where $D(x)$ is the density of states. We approximate $D(x)$ by $D(E_F)$ in the narrow range of integration and obtain (Problem 14.10)

$$E = 2E_F - \frac{2\hbar\omega_\mathbf{q}\exp[-2/D(E_F)U]}{1 - \exp[-2/D(E_F)U]} \approx 2E_F - 2\hbar\omega_\mathbf{q}\exp[-2/D(E_F)U]. \tag{14.84}$$

The expression on the extreme right in Eq. (14.84) is valid for weak interactions (small U). We note that we have made the approximation $V_{\mathbf{kq}} = -U$ in the range of attractive interaction and zero elsewhere. Thus, the energy of the electron pair is less than $2E_F$ in the absence of the interaction. It can be shown that all other solutions lead to energies greater than $2E_F$. Hence, the lowest energy state of the electron pair is a bound state known as a Cooper pair (Ref. 7) that is formed from a pair of electrons with opposite spin and opposite wave vector.

The formation of a bound state by the additional electron pair means that when two electrons from states directly below the Fermi surface are excited into states above it, the energy is lowered. Thus, the filled Fermi sphere is unstable, and one can gain energy by combining electrons into Cooper pairs.

14.7.4 BCS Theory

The theory of superconductivity was proposed by Bardeen, Cooper, and Schrieffer on the basic assumption that electron–phonon interaction provides a means for creating Cooper pairs.[2] A ground state of a superconductor consists of a condensate, which is a single quantum state available only to interacting Cooper pairs. The condensate is the product of the pair wave functions, and its center of mass is stationary in the absence of electric and magnetic fields. If one wants to remove a pair of electrons from the condensate, an energy 2Δ (the binding energy of the Cooper pair) is required to "break" a pair.

The BCS model Hamiltonian (Ref. 2) can be written as

$$\hat{H}_{BCS} = \sum_{\mathbf{k},s} E_\mathbf{k}\hat{c}_{\mathbf{k}s}^\dagger\hat{c}_{\mathbf{k}s} + \sum_{\mathbf{kk}'} U_{\mathbf{kk}'}\hat{c}_{\mathbf{k}\uparrow}^\dagger\hat{c}_{-\mathbf{k}\downarrow}^\dagger\hat{c}_{-\mathbf{k}'\downarrow}\hat{c}_{\mathbf{k}'\uparrow}. \tag{14.85}$$

Bardeen et al.[2] used the grand canonical ensemble and showed that the wave function for coherent states can be written as

$$|\Phi> = \prod_\mathbf{k}[1 + g_\mathbf{k}\hat{c}_{\mathbf{k}\uparrow}^\dagger\hat{c}_{-\mathbf{k}\downarrow}^\dagger]|\Theta> = \hat{\Phi}|\Theta>, \tag{14.86}$$

which creates all possible pairs of $2N$ particles with various weights through $g_\mathbf{k}$. They used a variational procedure by using the constraint that the average particle number is maintained at N. However, we will use the Bogoliubov–Valatin transformation and obtain the same result as the BCS theory.[5]

14.7.5 Ground State of the Superconducting Electron Gas

We can write the Hamiltonian in Eq. (14.75) in a simpler form,

$$H = \sum_\mathbf{k} E(\mathbf{k})(\hat{c}_\mathbf{k}^\dagger\hat{c}_\mathbf{k} + \hat{c}_{-\mathbf{k}}^\dagger\hat{c}_{-\mathbf{k}}) - U\sum_{\mathbf{kk}'} \hat{c}_{\mathbf{k}'}^\dagger\hat{c}_{-\mathbf{k}'}^\dagger\hat{c}_{-\mathbf{k}}\hat{c}_\mathbf{k}, \tag{14.87}$$

where a positive spin is associated with the index $\mathbf{k}$, and a negative spin is associated with the index $-\mathbf{k}$. Eq. (14.87) is rearranged by introducing the following creation and annihilation operators:

$$\hat{\alpha}_{\mathbf{k}} = u_{\mathbf{k}}\hat{c}_{\mathbf{k}} - v_{\mathbf{k}}\hat{c}_{-\mathbf{k}}^{\dagger}$$
$$\hat{\alpha}_{-\mathbf{k}} = u_{\mathbf{k}}\hat{c}_{-\mathbf{k}} + v_{\mathbf{k}}\hat{c}_{\mathbf{k}}^{\dagger}$$
$$\hat{\alpha}_{\mathbf{k}}^{\dagger} = u_{\mathbf{k}}\hat{c}_{\mathbf{k}}^{\dagger} - v_{\mathbf{k}}\hat{c}_{-\mathbf{k}}$$
$$\alpha_{-\mathbf{k}}^{\dagger} = u_{\mathbf{k}}c_{-\mathbf{k}}^{\dagger} + v_{\mathbf{k}}\hat{c}_{\mathbf{k}}. \tag{14.88}$$

In the preceding transformations, we use the conditions $u_{\mathbf{k}}^2 + v_{\mathbf{k}}^2 = 1$, $u_{\mathbf{k}} = u_{-\mathbf{k}}$, $v_{\mathbf{k}} = -v_{-\mathbf{k}}$. In addition, $u_{\mathbf{k}}$ and $v_{\mathbf{k}}$ are nonzero outside and inside the Fermi sphere, respectively. These conditions guarantee that the commutation relations for the $\hat{c}-$ operators also apply to the $\hat{\alpha}-$ operators (Problem 14.11). We avoid the confusion created by the situation that a hole in the state $\mathbf{k}$ has a momentum $-\hbar\mathbf{k}$ while an electron has a momentum $\hbar\mathbf{k}$ by defining quasi-particles which have momentum $\hbar\mathbf{k}$ both outside and inside the Fermi sphere. Since a quasi-particle of momentum $\hbar\mathbf{k}$ is created by the operator $c_{\mathbf{k}}^{\dagger}$ when it is outside the Fermi sphere and by $c_{-\mathbf{k}}$ when it is inside the Fermi sphere, we have in Eq. (14.88),

$$u_{\mathbf{k}} = 1, v_{\mathbf{k}} = 0 \quad \text{for} \quad k > k_F$$
$$u_{\mathbf{k}} = 0, v_{\mathbf{k}} = 1 \quad \text{for} \quad k < k_F. \tag{14.88a}$$

We also introduce the operator $\overline{\hat{H}} = \hat{H} - E_F\hat{N}$ and the energy $\varepsilon(\mathbf{k}) = E(\mathbf{k}) - E_F$. The transition from the $\hat{c}-$ to the $\hat{\alpha}-$ operators (Bogoliubov–Valatin transformation) leads to (Problem 14.12)

$$\begin{aligned}
\overline{\hat{H}} = \sum_{\mathbf{k}} \varepsilon(\mathbf{k})&[2v_{\mathbf{k}}^2 + (u_{\mathbf{k}}^2 - v_{\mathbf{k}}^2)(\hat{\alpha}_{\mathbf{k}}^{\dagger}\hat{\alpha}_{\mathbf{k}} + \hat{\alpha}_{-\mathbf{k}}^{\dagger}\hat{\alpha}_{-\mathbf{k}}) + 2u_{\mathbf{k}}v_{\mathbf{k}}(\alpha_{\mathbf{k}}^{\dagger}\hat{\alpha}_{-\mathbf{k}}^{\dagger} + \hat{\alpha}_{-\mathbf{k}}\hat{\alpha}_{\mathbf{k}})] \\
&- U\sum_{\mathbf{k}\mathbf{k}'}\{[u_{\mathbf{k}}v_{\mathbf{k}}u_{\mathbf{k}'}v_{\mathbf{k}'}(1 - \hat{\alpha}_{-\mathbf{k}'}^{\dagger}\hat{\alpha}_{-\mathbf{k}'} - \hat{\alpha}_{\mathbf{k}'}^{\dagger}\hat{\alpha}_{\mathbf{k}'})(1 - \hat{\alpha}_{-\mathbf{k}}^{\dagger}\hat{\alpha}_{-\mathbf{k}} - \hat{\alpha}_{\mathbf{k}}^{\dagger}\hat{\alpha}_{\mathbf{k}})] \\
&+ (u_{\mathbf{k}}^2 - v_{\mathbf{k}}^2)u_{\mathbf{k}'}v_{\mathbf{k}'}(1 - \hat{\alpha}_{-\mathbf{k}'}^{\dagger}\hat{\alpha}_{-\mathbf{k}'} - \hat{\alpha}_{\mathbf{k}'}^{\dagger}\hat{\alpha}_{\mathbf{k}'})(\hat{\alpha}_{-\mathbf{k}}\hat{\alpha}_{\mathbf{k}} + \hat{\alpha}_{\mathbf{k}}^{\dagger}\hat{\alpha}_{-\mathbf{k}}^{\dagger}) \\
&+ (u_{\mathbf{k}}^2\hat{\alpha}_{-\mathbf{k}}\hat{\alpha}_{\mathbf{k}} - v_{\mathbf{k}}^2\hat{\alpha}_{\mathbf{k}}^{\dagger}\alpha_{-\mathbf{k}}^{\dagger})(u_{\mathbf{k}'}^2\hat{\alpha}_{\mathbf{k}'}^{\dagger}\alpha_{-\mathbf{k}'}^{\dagger} - v_{\mathbf{k}'}^2\hat{\alpha}_{-\mathbf{k}'}\hat{\alpha}_{\mathbf{k}'})\}. \tag{14.89}
\end{aligned}$$

The last term of the first line in Eq. (14.89) vanishes from the condition that $u_{\mathbf{k}}$ and $v_{\mathbf{k}}$ are zero inside and outside the Fermi sphere (Eq. 14.88 (a)). Normally, the first term (energy of the filled Fermi sphere) and the second term (energy of the quasiparticles defined by $\alpha_{\mathbf{k}}^{\dagger}\alpha_{\mathbf{k}}$) remain, but in the ground state, the second term vanishes. As we will show, the terms containing the products of $\alpha_{\mathbf{k}}^{\dagger}\alpha_{-\mathbf{k}}^{\dagger}$ and $\alpha_{-\mathbf{k}}\alpha_{\mathbf{k}}$ can be eliminated by choosing different values of $u_{\mathbf{k}}$ and $v_{\mathbf{k}}$. The last term in Eq. (14.89) contributes very little to the final result and hence can be neglected.

Thus, in the ground state, Eq. (14.89) can be rewritten as

$$\overline{H}_G = 2\sum_{\mathbf{k}} \varepsilon(\mathbf{k})v_{\mathbf{k}}^2 - U\sum_{\mathbf{k},\mathbf{k}'} u_{\mathbf{k}}v_{\mathbf{k}}u_{\mathbf{k}'}v_{\mathbf{k}'} + \sum_{\mathbf{k}}\left[2u_{\mathbf{k}}v_{\mathbf{k}}\varepsilon(\mathbf{k}) - (u_{\mathbf{k}}^2 - v_{\mathbf{k}}^2)U\sum_{\mathbf{k}'}u_{\mathbf{k}'}v_{\mathbf{k}'}\right](\hat{\alpha}_{\mathbf{k}}^{\dagger}\hat{\alpha}_{-\mathbf{k}}^{\dagger} + \hat{\alpha}_{-\mathbf{k}}\hat{\alpha}_{\mathbf{k}}). \tag{14.90}$$

For the square bracket in Eq. (14.90) to vanish, we first introduce a constant,

$$\Delta = U\sum_{\mathbf{k}} u_{\mathbf{k}}v_{\mathbf{k}}, \tag{14.91}$$

and then set the condition,

$$2u_{\mathbf{k}}v_{\mathbf{k}}\varepsilon(\mathbf{k}) = \Delta(u_{\mathbf{k}}^2 - v_{\mathbf{k}}^2). \tag{14.92}$$

In addition,

$$u_{\mathbf{k}}^2 + v_{\mathbf{k}}^2 = 1. \tag{14.93}$$

From Eqs. (14.92) and (14.93), it is easy to show that

$$\xi_{\mathbf{k}} = \frac{\varepsilon(\mathbf{k})}{\sqrt{\varepsilon^2(\mathbf{k}) + \Delta^2}}, \tag{14.94}$$

$$u_{\mathbf{k}}^2 = \frac{1}{2}(1 + \xi_{\mathbf{k}}) \\ v_{\mathbf{k}}^2 = \frac{1}{2}(1 - \xi_{\mathbf{k}}). \tag{14.95}$$

From Eqs. (14.91), (14.94), and (14.95), one can show (Problem 14.12)

$$\Delta = U\sum_{\mathbf{k}} u_{\mathbf{k}}v_{\mathbf{k}} = \frac{U}{2}\sum_{\mathbf{k}}\frac{\Delta}{\sqrt{\varepsilon^2(\mathbf{k}) + \Delta^2}}. \tag{14.96}$$

Because $\Delta \neq 0$ (no vanishing interaction), $U \neq 0$ only in the range $|\varepsilon(\mathbf{k})| \leq \hbar\omega_{\mathbf{q}}$. Since the sum is over one spin direction, the density of states is $D(\varepsilon)/2$. Thus, while converting the summation over $\mathbf{k}$ to an integration, we can write Eq. (14.96) in the alternate form

$$\frac{U}{4}\int_{-\hbar\omega_{\mathbf{q}}}^{\hbar\omega_{\mathbf{q}}}\frac{D(\varepsilon)d\varepsilon}{\sqrt{\varepsilon^2 + \Delta^2}} \approx \frac{UD(E_F)}{4}\int_{-\hbar\omega_{\mathbf{q}}}^{\hbar\omega_{\mathbf{q}}}\frac{d\varepsilon}{\sqrt{\varepsilon^2 + \Delta^2}} = 1. \tag{14.97}$$

We obtain from Eq. (14.97)

$$\Delta = 2\hbar\omega_{\mathbf{q}}\exp[-2/D(E_F)U]. \tag{14.98}$$

This is precisely the binding energy of the Cooper pair. Because the energy of the filled Fermi sphere is

$$\overline{H}_0 = 2\sum_{\mathbf{k} < \mathbf{k}_F}\varepsilon(\mathbf{k}), \tag{14.99}$$

from Eqs. (14.90) and (14.99), we obtain the difference between the Hamiltonians with and without interactions (note that the coefficient of the square bracket in Eq. 14.90 is equal to zero), which, in the absence of any operators, is the energy difference between the ground state of the interacting and noninteracting electron gas:

$$E = \overline{H}_G - \overline{H}_0 = 2\sum_{\mathbf{k}}\varepsilon(\mathbf{k})v_{\mathbf{k}}^2 - 2\sum_{\mathbf{k} < \mathbf{k}_F}\varepsilon(\mathbf{k}) - U\sum_{\mathbf{k}\mathbf{k}'}u_{\mathbf{k}}v_{\mathbf{k}}u_{\mathbf{k}'}v_{\mathbf{k}'}. \tag{14.100}$$

Substituting the values of $u_{\mathbf{k}}$, $v_{\mathbf{k}}$, and $\xi_{\mathbf{k}}$ from Eqs. (14.94) and (14.95) in Eq. (14.100), we obtain

$$E = \sum_{\mathbf{k}<\mathbf{k}_F} |\varepsilon| \left(1 - \frac{|\varepsilon|}{\sqrt{\varepsilon^2 + \Delta^2}}\right) + \sum_{\mathbf{k}>\mathbf{k}_F} \varepsilon \left(1 - \frac{\varepsilon}{\sqrt{\varepsilon^2 + \Delta^2}}\right) - \sum_{\mathbf{k}} \frac{\Delta^2}{2\sqrt{\varepsilon^2 + \Delta^2}}. \tag{14.101}$$

When we convert the sum over $\mathbf{k}$ to an integration (with only one spin direction),

$$E = D(E_F) \int_0^{\hbar\omega_{\mathbf{q}}} \left(\varepsilon - \frac{1}{2}\frac{2\varepsilon^2 + \Delta^2}{\sqrt{\varepsilon^2 + \Delta^2}}\right) d\varepsilon. \tag{14.102}$$

After integrating Eq. (14.102) (see Problem 14.13), we obtain for weak interactions, $(\Delta \ll \hbar\omega_{\mathbf{q}})$,

$$E = \frac{D(E_F)}{2}(\hbar\omega_{\mathbf{q}})^2 \left[1 - \sqrt{1 + \left(\frac{\Delta}{\hbar\omega_{\mathbf{q}}}\right)^2}\right] \approx -\frac{D(E_F)\Delta^2}{4}. \tag{14.103}$$

E is known as the condensate energy of the ground state.

14.7.6 Excited States at $T = 0$

From Eqs. (14.89) and (14.90), we can write the Hamiltonian of the excited states, $\overline{H}_e$, as

$$\overline{H}_e = \overline{H}_G + \sum_{\mathbf{k}} \left[\varepsilon(\mathbf{k})(u_{\mathbf{k}}^2 - v_{\mathbf{k}}^2) + U\sum_{\mathbf{k}'} 2u_{\mathbf{k}}v_{\mathbf{k}}u_{\mathbf{k}'}v_{\mathbf{k}'}\right]\left(\hat{\alpha}_{\mathbf{k}}^\dagger\hat{\alpha}_{\mathbf{k}} + \hat{\alpha}_{-\mathbf{k}}^\dagger\hat{\alpha}_{-\mathbf{k}}\right) + \cdots. \tag{14.104}$$

Eq. (14.104) can be expressed by using Eq. (14.91),

$$\overline{H}_e = \overline{H}_G + \sum_{\mathbf{k}} \left[\varepsilon(\mathbf{k})(u_{\mathbf{k}}^2 - v_{\mathbf{k}}^2) + 2\Delta u_{\mathbf{k}}v_{\mathbf{k}}\right]\left(\hat{\alpha}_{\mathbf{k}}^\dagger\hat{\alpha}_{\mathbf{k}} + \hat{\alpha}_{-\mathbf{k}}^\dagger\hat{\alpha}_{-\mathbf{k}}\right) + \cdots. \tag{14.105}$$

Eq. (14.105) can be rewritten with the help of Eq. (14.92),

$$\overline{H}_e = \overline{H}_G + \sum_{\mathbf{k}} \frac{2u_{\mathbf{k}}v_{\mathbf{k}}}{\Delta}\left(\varepsilon^2(\mathbf{k}) + \Delta^2\right)(n_{\mathbf{k}\uparrow} + n_{-\mathbf{k}\downarrow}). \tag{14.106}$$

From Eqs. (14.96) and (14.106), we obtain

$$E - E_0 = \sum_{\mathbf{k}} \left[\varepsilon^2(\mathbf{k}) + \Delta^2\right]^{1/2} n_{\mathbf{k}}. \tag{14.107}$$

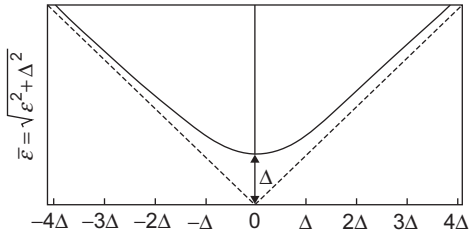The energy of a quasiparticle is given by

$$\overline{\varepsilon}(\mathbf{k}) = \sqrt{\varepsilon^2(\mathbf{k}) + \Delta^2}. \tag{14.108}$$

Note that here the energy $\varepsilon(\mathbf{k})$ is measured from the Fermi surface:

$$\varepsilon(\mathbf{k}) = E(\mathbf{k}) - E_F. \tag{14.109}$$

Thus, the ground and the first excited states are separated by an energy gap Δ. This is shown in Figure 14.13.

FIGURE 14.13

Energy $\bar{\varepsilon}(\mathbf{k})$ of the quasiparticles plotted as a function of $\varepsilon(\mathbf{k}) = E(\mathbf{k}) - E_F$.

Because in a scattering process, a quasi-particle is created in pairs, corresponding to the electron-hole pair of the noninteracting electron gas, the threshold energy of an excitation is 2Δ. This leads to the conclusion that the Cooper pairs must be broken up during the scattering process. Thus, both Cooper pairs and single quasiparticles are present in the excited state, and while individual particles are scattered, Cooper pairs lead to a current that flows without resistance. We now are back to a two-fluid model.

14.7.7 Excited States at $T \neq 0$

The states $\mathbf{k}\uparrow$ and $\mathbf{k}\downarrow$ are fermions, and at temperatures $T \neq 0$, replacing the particle numbers $n_{\mathbf{k}}$ by their statistical average, we obtain by taking the Fermi distribution as the occupational probability,

$$<n_{\mathbf{k}}> \equiv f_{\mathbf{k}} = \frac{1}{e^{\beta\bar{\varepsilon}(\mathbf{k})} + 1}, \tag{14.110}$$

where the energy of the quasiparticles $\bar{\varepsilon}(\mathbf{k})$ replaces the usual energy difference $E - \mu$. We further note that $\bar{\varepsilon}(\mathbf{k})$ is always positive (from Eq. 14.108), except that $\varepsilon(\mathbf{k})$ is defined as $\varepsilon(\mathbf{k}) = E(\mathbf{k}) - \mu$ at $T \neq 0$. Because $n_{\mathbf{k}} \neq 0$ for $T \neq 0$, the energy gap Δ is now temperature dependent, $\Delta(T)$. Thus, the bracket in Eq. (14.90) has to be replaced by the condition

$$2u_{\mathbf{k}}v_{\mathbf{k}}\varepsilon(\mathbf{k}) - (u_{\mathbf{k}}^2 - v_{\mathbf{k}}^2)U\sum_{\mathbf{k}'} u_{\mathbf{k}'}v_{\mathbf{k}'}(1 - 2f_{\mathbf{k}'}) = 0. \tag{14.111}$$

Similarly, $\Delta(T)$ is defined as

$$\Delta(T) = U\sum_{\mathbf{k}'} u_{\mathbf{k}'}v_{\mathbf{k}'}(1 - 2f_{\mathbf{k}'}) = \frac{U}{2}\sum_{\mathbf{k}'} \frac{\Delta(T)}{\sqrt{\varepsilon^2(\mathbf{k}') + \Delta^2(T)}}(1 - 2f_{\mathbf{k}'}). \tag{14.112}$$

Because the critical temperature T_c is the highest one for which Eq. (14.112) has a solution for which $\Delta(T) \neq 0$, and the sum over $\mathbf{k}'$ is over one spin state, we can eliminate $\Delta(T)$ from both sides, and by using a procedure similar to Eq. (14.97), we obtain

$$\frac{UD(E_F)}{4} \int_{-\hbar\omega_{\mathbf{q}}}^{\hbar\omega_{\mathbf{q}}} \frac{d\varepsilon}{\sqrt{\varepsilon^2 + \Delta^2(T)}} \left\{ 1 - 2f\left(\frac{\sqrt{\varepsilon^2 + \Delta^2(T)}}{k_B T}\right) \right\} = 1. \tag{14.113}$$

Eq. (14.113) can be rewritten in the alternate form

$$\int_{-\hbar\omega_{\mathbf{q}}}^{\hbar\omega_{\mathbf{q}}} \frac{d\varepsilon}{\sqrt{\varepsilon^2 + \Delta^2(T)}} - \int_{-\hbar\omega_{\mathbf{q}}}^{\hbar\omega_{\mathbf{q}}} \frac{d\varepsilon}{\sqrt{\varepsilon^2 + \Delta^2(T)}} 2f\left(\frac{\sqrt{\varepsilon^2 + \Delta^2(T)}}{k_B T}\right) = \frac{4}{UD(E_F)}. \tag{14.114}$$

Because $\Delta(0) \ll \hbar\omega_{\mathbf{q}}$, it can be shown from Eqs. (14.98) and (14.114) that (Problem 14.14)

$$\ln\frac{\Delta(T)}{\Delta(0)} = -2\int\limits_0^\infty \frac{dx}{\sqrt{x^2+1}} f\left(\sqrt{x^2+1}\,\frac{\Delta(T)}{\Delta(0)}\left[\frac{k_BT}{\Delta(0)}\right]^{-1}\right) = F\left(\frac{\Delta(T)}{\Delta(0)},\frac{k_BT}{\Delta(0)}\right). \tag{14.115}$$

Because Eq. (14.115) is a function of two parameters $\Delta(T)/\Delta(0)$ and $k_BT/\Delta(0)$, T_c is calculated from the condition that $\Delta(T_c) = 0$ is linearly dependent on $\Delta(0)$. It can be shown by numerical integration that

$$k_BT_c \approx 0.57\Delta(0). \tag{14.116}$$

Eq. (14.116) can be rewritten in the alternate form

$$\frac{2\Delta(0)}{k_BT_c} \approx 3.53. \tag{14.117}$$

Approximating $\omega_{\mathbf{q}}$ by ω_D (the Debye frequency), replacing the Debye temperature $\theta_D = \hbar\omega_D/k_B$, from Eqs. (14.98) and (14.117), we obtain

$$T_c \approx 1.13\,\theta_D\,\exp\left[-\frac{2}{D(E_F)U}\right]. \tag{14.118}$$

[Be aware that in the notations of BCS theory, $N(E_F) = D(E_F)/2$ is the density of states per spin and $U=V$.]

The BCS theory of superconductivity (Ref. 2) can be briefly summarized as follows. When a uniform electric field is applied to a superconductor, a current is generated because all the pairs in the condensate experience the same force and move in the same direction. When a voltage difference V exists across the two ends of the superconductor, an energy $2\,eV$ would be gained by a Cooper pair and different parts of the condensate would have different energy, and eventually, the condensate would be lost. Thus, the condensate must move and carry current without any potential difference; i.e., it must exist as a phase-locked entity. The condensate cannot receive any energy less than $2\Delta(T)$, the energy required to break a single pair of the condensate. However, when the temperature is above zero, some pairs are broken due to thermal excitation. Because the density of Cooper pairs is large at absolute zero, the initial reduction of numbers has little effect on 2Δ, but as T approaches a critical temperature $T = T_c$, $2\Delta(T_c) = 0$ and the condensate ceases to exist. The Cooper pairs are broken into individual electrons, and superconductivity is destroyed. A diagram that displays the reduced energy gap $\Delta(T)/\Delta(0)$ as a function of the reduced temperature T/T_c is shown in Figure 14.14.
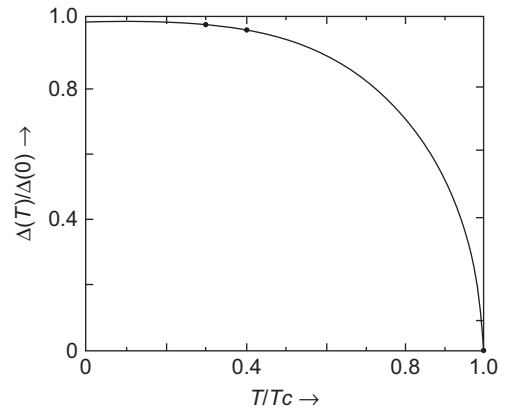

FIGURE 14.14

Reduced energy gap $\Delta(T)/\Delta(0)$ as a function of reduced temperature T/T_c.

It can also be shown that the condensation energy per unit volume is given by

$$W = -1/4 \, D(E_F)\Delta^2. \tag{14.119}$$

If we distinguish the density of states in a normal conductor as $D_n(E)dE$ and in its superconducting state as $D_s(\overline{\varepsilon}(\mathbf{k}))d\overline{\varepsilon}(\mathbf{k})$, where $\overline{\varepsilon}(\mathbf{k}) = E - E_F$ (Eq. 14.108), because no states are lost,

$$D_n(E)dE = D_s(\overline{\varepsilon}(\mathbf{k}))d\overline{\varepsilon}(\mathbf{k}), \tag{14.120}$$

from which we obtain

$$D_s(\overline{\varepsilon}) = D_n(E)\frac{dE}{d\overline{\varepsilon}}. \tag{14.121}$$

Eq. (14.121) can be rewritten in the alternate form by using Eqs. (14.108) and (14.109),

$$
\begin{aligned}
D_s(\overline{\varepsilon}) &= D_n(E)\,\frac{\overline{\varepsilon}}{(\overline{\varepsilon}^2 - \Delta^2)^{1/2}}, & |\overline{\varepsilon}| > \Delta, \\
&= 0, & |\overline{\varepsilon}| < 0.
\end{aligned}
\tag{14.122}
$$

14.8 STRONG-COUPLING THEORY

14.8.1 Introduction

The BCS theory is based on a weak coupling approximation, i.e., the electron–phonon coupling constant $\lambda \ll 1$ at $T = 0$. Here, λ reflects the strength of the electron–lattice interaction. However, for many superconductors, $\lambda \geq 1$. For example, $\lambda = 1.4$ for lead, $\lambda = 1.6$ for mercury, and $\lambda = 2.1$ for $Pb_{0.65}Bi_{0.35}$. Thus, the more universal approach of the strong-coupling theory was developed after the formulation of the BCS theory. The strong-coupling theory is based on the Green's function method of the many-body theory, and we will introduce only the main results of this theory as derived by McMillan[21] and modified by Dynes (Ref. 11).

14.8.2 Upper Limit of the Critical Temperature, T_c

The electron–phonon coupling constant can be written as

$$\lambda = 2\int\alpha^2(\Omega)F(\Omega)\Omega^{-1}d\Omega, \tag{14.123}$$

where Ω is the phonon frequency (we note that $\hbar\Omega_D = k_B\theta_D$), $F(\Omega)$ is the phonon density of states, and $\alpha^2(\Omega)$ is a measure of the phonon-frequency-dependent electron–phonon interaction. The characteristic phonon frequency $\widetilde{\Omega}$ is defined as

$$\widetilde{\Omega} = <\Omega^2>^{1/2}, \tag{14.124}$$

where the average is determined by

$$<f(\Omega)> = \frac{2}{\lambda}\int f(\Omega)\alpha^2(\Omega)F(\Omega)d\Omega. \tag{14.125}$$

McMillan (Ref. 21) introduced a convenient expression for the coupling constant, λ,

$$\lambda = \nu <I^2>/M\overline{\Omega}^2, \tag{14.126}$$

where ν is the bulk density of states,

$$\nu = m^* p_F/2\pi^2, \tag{14.127}$$

and $<I^2>$ contains the average value of the electron–phonon matrix element I. The expression in the strong-coupling limit, for the critical temperature T_c, obtained by McMillan[21] (later modified by Dynes (Ref. 11)) is given by

$$T_c = \frac{\theta_D}{1.2}\exp\left[-\frac{1.04(1+\lambda)}{\lambda - \mu^*(1+0.62\lambda)}\right], \tag{14.128}$$

and μ^* can be expressed as the Coulombic pseudopotential $(\varepsilon_0 \approx E_F)$,

$$\mu^* = V_c[1 + V_c \ln(\varepsilon_0/\widetilde{\Omega})]^{-1}. \tag{14.129}$$

When we use a rough estimate of upper limit, each of these values is $\theta_D \approx 400°$ K, $\lambda \approx 0.8$, and $\mu^* \approx 0.1$. In Eq. (14.128), we obtain the upper limit for $T_c \approx 30°$ K in the strong coupling limit. In fact, until 1986, Nb_3Ge was the material that had the highest critical temperature, $T_c = 23°$ K.

14.9 HIGH-TEMPERATURE SUPERCONDUCTORS

14.9.1 Introduction

A new class of superconducting materials, the high T_c copper oxides (often called cuprates), was discovered by Bednroz and Muller in 1986.[3] They found that $La_{1.85}Ba_{0.15}CuO_4$ became superconducting at a critical temperature of $T_c \approx 30°$ K. The atomic structure of this remarkable superconductor is shown in Figure 14.15.

$La_{1.85}Ba_{0.5}CuO_4$ is very different from traditional superconductors in the sense that it is not a conventional metal but brittle ceramic, which is an antiferromagnetic insulator, carefully doped so as to produce metallic and superconducting phases. The discovery of $La_{1.85}Ba_{0.15}CuO_4$ set out a frenzy to discover more high T_c superconductors. The synthesis of the similar compound $La_{1.82}Sr_{0.18}CuO_4$ moved the transition temperature close to $T_c \approx 40°$ K. The first high-temperature superconductor of which the critical temperature exceeded the liquid nitrogen temperature is

● La, Ba • Cu ○ O

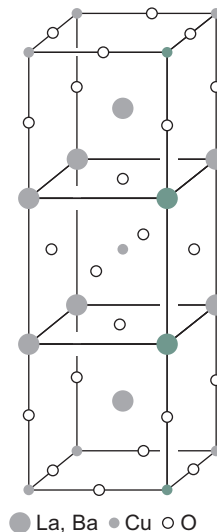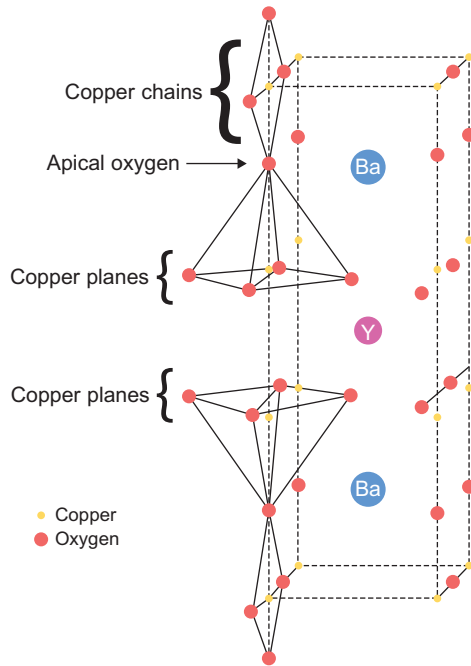**FIGURE 14.15**

The atomic structure of $La_{1.85}Ba_{0.15}CuO_4$.

FIGURE 14.16

Structure of the YBCO compound.

Reproduced from Kresin and Wolf[16] with the permission of the American Physical Society.

$YBa_2Cu_3O_{7-x}$ ($x = 0.1$) with $T_c \approx 93°$ K, which was discovered by Wu et al.[29] in February 1987. In fact, it was soon found that $YBa_2Cu_3O_{7-x}$ is superconducting in the orthogonal structure ($0 \le x \le 0.6$) although it is not superconducting in the tetragonal structure ($x > 0.6$). This is the most studied high T_c compound. The orthogonal YBCO structure is shown in Figure 14.16. The highest observed value of T_c is 150° K for the $HgBa_2Ca_2Cu_3O_{8+x}$ compound under pressure.

14.9.2 Properties of Novel Superconductors (Cuprates)

All cuprates have a layered structure. The main structural unit typical for the whole family is the Cu-O plane (see Figure 14.16), where the pairing originates and the charge reservoir is located. The YBCO compound contains the Cu-O chains, and the change in the oxygen content in the chain layers leads to charge transfer between these two subsystems. The charge transfer occurs through the apical oxygen ion located between the chains and the planes, as shown in Figure 14.16.

Whereas the undoped parent compounds of the cuprates are insulators, the novel superconductors are doped materials. Doping leads to conductivity and, for larger concentration, to superconductivity. The doping is provided either by changing the oxygen content or by chemical substitution (La $\rightarrow$ Sr substitution in $La_{2-x}Sr_xCuO_4$). The dopants create electrons, whereas the holes are produced by doping, which removes electrons. For example, some cuprates like YBCO contain carriers that are holes, whereas other cuprates like Nd-Ce-Cu-O contain carriers that are electrons. The maximum value of $T_c \equiv T_c^{max}$ is obtained for a characteristic value n_m of the carrier concentration. $T_c < T_c^{max}$ for both $n < n_m$ (the underdoped region) and $n > n_m$ (the overdoped region).

14.9.3 Brief Review of *s*-, *p*-, and *d*-wave Pairing

Next, we will review the three possible choices for pairing—the *s*-, *p*-, and *d*-wave pairings—and discuss the differences between these types of pairings. The Landau–Ginzburg (Ref. 17) order parameter $\Psi(\mathbf{r})$ (defined in Eq. 14.17) becomes nonzero only in the presence of superconductivity. Under a gauge transformation,

$$\mathbf{A} \rightarrow \mathbf{A} + \overrightarrow{\nabla}\phi, \tag{14.130}$$

$$\Psi \rightarrow \Psi e^{-2ie\phi/\hbar c}. \tag{14.131}$$

In fact, Gorkov showed that the pair potential $\Delta_{\mathbf{r}}$ (used in Bogoliubov theory of superconductivity) is proportional to the order parameter $\Psi(\mathbf{r})$ and also transforms as

$$\Delta_{\mathbf{r}} \to \Delta_{\mathbf{r}} e^{-2ie\phi/\hbar c}. \tag{14.132}$$

The implicit assumption in the BCS theory of superconductivity was that the effective potential U was isotropic and $\Psi(\mathbf{r})$ depended only on the center-of-mass coordinate $\mathbf{r} = (\mathbf{r} + \mathbf{r}')/2$. This is known as s-wave superconductivity. However, in general, the order parameter is a function of $\Psi(\mathbf{r}, \mathbf{r}')$, and one can define $\mathbf{R} = \mathbf{r} - \mathbf{r}'$. When Ψ is independent of the direction of $\mathbf{R}$, the superconductor is called s-wave. When Ψ decays rapidly as a function of $\mathbf{R}$, Ψ has the symmetry of $\overrightarrow{x} \cdot \mathbf{R}$ (proportional to $\cos\theta$, as in the case of superfluid ^{3}He); this is called p-wave. When Ψ depends on the direction of $\mathbf{R}$, the symmetry is $(\overrightarrow{x} \cdot \mathbf{R})^2 - (\overrightarrow{y} \cdot \mathbf{R})^2$, which is proportional to $\cos 2\theta$ and is known as d-wave.

One can also gain insight into the nature of the pair-condensate state based on symmetry considerations. For example, the parity of a superconductor with inversion symmetry can be specified using the Pauli exclusion principle. Because the crystal structures of bulk superconductors are all characterized by a center of inversion, they can be classified by the parity of the pair state. The spin-triplet state (total spin $S = 1$) has a superconducting order parameter (gap function) with odd parity, while the spin-singlet pair state ($S = 0$) corresponds to an orbital pair wave function $\psi(\mathbf{k}) \propto \Delta(\mathbf{k})$ with even parity, i.e., $\Delta(\mathbf{k}) = \Delta(-\mathbf{k})$. Because spin-orbit interaction is relatively small in cuprate superconductors, the spin-singlet and -triplet states are well defined. It can be shown from group-theoretical considerations that the gap function $\Delta(\mathbf{k})$ for each pair state can be expanded as a function of k_x, k_y, and k_z. Some examples follow:

$$\Delta_s(\mathbf{k}) = \Delta_s^0 + \Delta_s^1(\cos k_x + \cos k_y) + \Delta_s^2 \cos k_z + \cdots, \tag{14.133}$$

$$\Delta_{d_{x^2-y^2}}(\mathbf{k}) = \Delta_{d_{x^2-y^2}}^0(\cos k_x - \cos k_y) + \cdots, \tag{14.134}$$

$$\Delta_{d_{xy}}(\mathbf{k}) = \Delta_{d_{xy}}^0(\sin k_x \sin k_y) + \cdots. \tag{14.135}$$

Thus, the order parameters for both the possible d-wave pair states have node lines.

All cuprate superconductors are characterized by a relatively high ratio of c-axis to a-axis lattice constants. For example, the c/a ratio is 3.0 for YBCO, 5.7 for BI-2212, and 7.6 for Tl-2212. These ratios of c/a translate into a flattened Brillouin zone possessing the basic symmetric properties of the unit cell of a square/rectangular lattice. Recent studies of interplane dc and ac intrinsic Josephson effects has shown that high T_c superconductors such as Bi-2212 act as stacks of two-dimensional superconducting CuO_2-based layers coupled by Josephson interactions (Ref. 13). It has also been shown that the vortex state can be understood in terms of stacks of two-dimensional pancake vortices. The cores of these 2D vortices, localized in the CuO_2 layers, are connected by Josephson vortices with cores confined in the nonsuperconducting charge-reservoir layers (see Figure 14.16). Thus, the pairing symmetry should reflect the underlying CuO_2 square/rectangular lattices. It is more convenient to consider our study of pairing symmetry in a square lattice. A $\mathbf{k}$-space representation of allowed symmetry basis functions for the C_{4v} symmetry is shown in Figure 14.17.
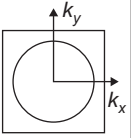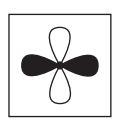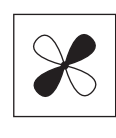
Group-theoretic notation	A_{1g}	A_{2g}	B_{1g}	B_{2g}
Order parameter basis function	constant	$xy(x^2-y^2)$	x^2-y^2	xy
Wave function name	s-wave	g	$d_{x^2-y^2}$	d_{xy}
Schematic representation of $\Delta(\mathbf{k})$ in B.Z.				

FIGURE 14.17

A **k**-space representation of allowed symmetry basis functions for the C_{4v} symmetry.

Reproduced from Tsuei and Kirtley[27] with the permission of the American Physical Society.

A schematic presentation in **k** space is shown where black and white represent opposite signs of the order parameter.

14.9.4 Experimental Confirmation of *d*-wave Pairing

Angle-Resolved Photoemission

A number of both non-phase-sensitive and phase-sensitive experimental techniques confirm that pairing in cuprates is highly anisotropic with a line of nodes in the superconducting gap. We will first discuss the angle-resolved photoemission spectroscopy (ARPES), which has the advantage of directly investigating the momentum space of the gap. We will discuss $Bi_2Sr_2CaCu_2O_{8+x}(Bi-2212)$, of which the complex structure consists of a superlattice of orthorhombic units. However, the basic orthorhombic subunit of $Bi_2Sr_2CaCu_2O_{8+x}(Bi-2212)$ has essentially tetragonal symmetry with lattice parameters $a \approx b$. This pseudotetragonal subunit is closely approximated by a body-centered tetragonal structure of which the primitive cell is shown in Figure 14.18. The key elements of this structure are the presence of two Cu-O sheets similar to those in the 40° and 90° K materials, as well as a double layer of edge-sharing Bi-O octahedrals,
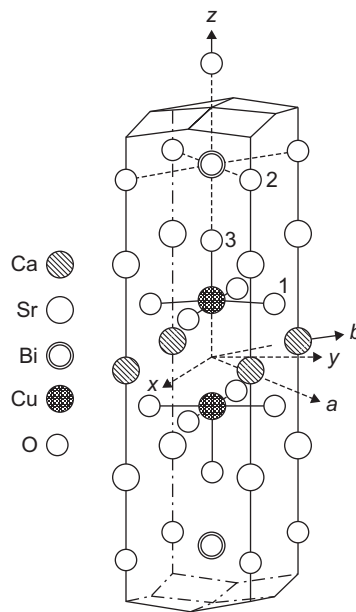

FIGURE 14.18

Primitive cell for body-centered tetragonal $Bi_2Sr_2CaCu_2O_{8+x}$. O(1), O(2), and O(3) denote oxygens in the Cu, Bi, and Sr planes, respectively. The *a* and the *b* axes at 45° to *x* and *y* are shown.

Reproduced from Stavola et al.[25] with the permission of the American Physical Society.

which fulfill a structural role that is analogous to the Cu-O chains in $YBa_2Cu_3O_7$. The main band features at the Fermi level include a pair of half-filled two-dimensional Cu-O $3d-2p$ bands similar to those found in other Cu-O planar superconductors, as well as slightly filled $6p$ bands, which provide additional carriers in the Bi-O planes.

The ARPES study shows that the gap in $Bi_2Sr_2CaCu_2O_{8+x}$(Bi−2212) (Ref. 10) is largest along the $\Gamma - M$ direction (parallel to a or b) and smallest among $\Gamma - Y$ (the diagonal line between them), as expected for a $d_{x^2-y^2}$ superconductor. Figure 14.19 shows the inferred value of the energy gap as a function of the angle in the Fermi surface (solid circles), compared to the prediction of a simple d-wave model (solid line). There is remarkable agreement between experimental and theoretical results. However, ARPES is not phase-sensitive and cannot distinguish between d-wave and highly anisotropic s-wave pairing.

Nuclear Magnetic Resonance

Nuclear-magnetic-resonance (NMR) measurements can probe the electronic properties of individual atomic sites on the CuO_2 sheets of the high-temperature superconductors. There is no

FIGURE 14.19

Energy gap in Bi − 2212, measured with ARPES as a function of an angle in the Fermi surface: solid curve, with fits to the data using a d-wave order parameter. Inset indicates the data points in the Brillouin zone.

Reproduced from Ding et al.[10] with permission of the American Physical Society.

Hebel-Slichter peak (found in normal superconductors due to density of states in the gap edge) and an increase in the nuclear relaxation rate T_1^{-1} near T_c, for both Cu and O in-plane sites. These properties can be explained by using a $d_{x^2-y^2}$ model with Coulomb correlations that yield (a) a weaker quasiparticle density-of-states singularity at the gap edge compared with an s-wave BCS gap, (b) the vanishing of the coherence factor for quasiparticle scattering for $\mathbf{q} \sim (\pi, \pi)$ for a $d_{x^2-y^2}$ gap, and (c) inelastic–scattering suppression of the peak, which is similar for both d-waves and s-waves. There has been excellent agreement between the experimental results for both the anisotropy ratio $(T_1^{-1})_{ab}/(T_1^{-1})_c$ and the transverse nuclear relaxation rate T_G^{-1} for $^{63}Cu(2)$ when a d-wave model is used, but absolutely no agreement when an s-wave model is used for the theoretical calculations.

Josephson Tunneling

As we discussed earlier, Josephson first pointed out that Cooper pairs can flow through a thin insulating barrier between two superconductors.[13] A schematic representation of a Josephson tunnel junction between a pure $d_{x^2-y^2}$ superconductor on the left and a superconductor with some admixture of s in a predominantly $d_{x^2-y^2}$ state on the right is shown in Figure 14.20. The gap states align with the crystal-line axes, which are rotated by angles θ_L and θ_R with respect to the junction normals $\mathbf{n}_L$ and $\mathbf{n}_R$.
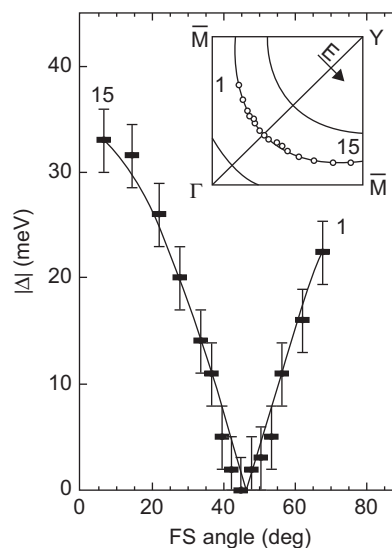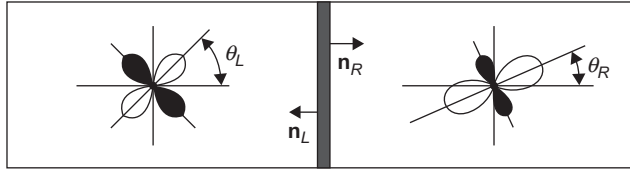
FIGURE 14.20

Schematic diagram of a Josephson junction showing the tunnel barrier sandwiched between two junction electrodes, with order parameters $\Delta_i(\mathbf{k}_i) = |\Delta_i|e^{i\phi_i}$.

Reproduced from Tsuei and Kirtley with the permission of the American Physical Society.[27]

The supercurrent I_s, proportional to the tunneling rate of Cooper pairs through the barrier, was given by Josephson as

$$I_s = I_c \sin\gamma, \tag{14.136}$$

where γ is the gauge-invariant phase difference at the junction,

$$\gamma = \phi_L - \phi_R + \frac{2\pi}{\Phi_0} \int\limits_L^R \mathbf{A} \cdot d\mathbf{l}, \tag{14.137}$$

where $\mathbf{A}$ is the vector potential, and $d\mathbf{l}$ is the element of line integration from the left electrode (L) to the right electrode (R) across the barrier. It was shown by Cohen et al. (Ref. 6) that the supercurrent I_s at zero temperature is given by

$$I_s = \sum_{\mathbf{k},\mathbf{l}} |T_{\mathbf{k},\mathbf{l}}|^2 \frac{\Delta_L(\mathbf{k})\Delta_R(\mathbf{l})}{E_L(\mathbf{k})E_R(\mathbf{l})} \frac{1}{[E_L(\mathbf{k}) + E_R(\mathbf{l})]} \sin(\gamma_L - \gamma_R), \tag{14.138}$$

where $T_{\mathbf{k},\mathbf{l}}$ is the time-reversal-symmetry-invariant tunneling matrix element,

$$E_i(\mathbf{k}) = \sqrt{\in_i^2(\mathbf{k}) + \Delta_i^2(\mathbf{k})}, \tag{14.139}$$

and $\in(\mathbf{k})$ is the one-electron energy. Eq. (14.138) is used to determine the parity of superconductors. It was shown by Pals et al. (Ref. 24). that I_s vanishes up to the second order in $T_{\mathbf{k},\mathbf{l}}$, in tunnel junctions between spin-singlet (even parity) and -triplet (odd parity) superconductors. However, because pair tunneling exists for Josephson junctions made of a cuprate superconductor and low-T_c conventional superconductor such as Nb or Pb, this confirms that the superconducting state in cuprates, just as in low-T_c conventional superconductors, is that of even-parity spin-singlet pairing.

π–Rings

The sign changes in the pair critical current I_c are arbitrary for a particular junction because an arbitrary phase can always be added to either side of the junction. However, the signs of the critical currents in a closed ring of superconductors that is interrupted by Josephson weak links can be assigned self-consistently. One can determine if a particular geometry is frustrated by counting these sign changes. A frustrated geometry has a local maximum in its free energy with zero

circulating supercurrent in the absence of an external magnetic field. A negative pair-tunneling critical current I_c can be considered as a phase shift of π at the junction interface, i.e.,

$$I_s = -|I_c| \sin \gamma = |I_c| \sin (\gamma + \pi). \tag{14.140}$$

A superconducting ring with an odd number of π shifts is frustrated.

In the Ginzburg–Landau formalism (Ref. 17), the order parameter is small near T_c, and hence, the free energy of the Josephson junction can be expanded as a power series of the order parameter. Further, the gap function can be expressed as a linear combination of the basis functions (χ_μ^j) of the irreducible representation (Γ^j), which corresponds to the highest T_c of the order parameter,

$$\Delta(\mathbf{k}) = \sum_{\mu=1}^{l_j} \eta_\mu \chi_\mu^j(\mathbf{k}), \tag{14.141}$$

where l_j is the dimensionality of Γ^j, and the expansion coefficient η_μ is invariant under all symmetry operations of the normal-state group G.

The free energy per unit area of Josephson coupling between two superconducting electrodes with order parameters ψ_L and ψ_R (Figure 14.20) can be written as

$$F_j = W \int ds \left[\psi_L \psi_R^* \exp \left[i(2\pi/\Phi_0) \int_L^R \mathbf{A} \cdot d\mathbf{l} \right] + c.c. \right], \tag{14.142}$$

where W is a measure of the Josephson coupling strength, and the integral is over the junction interface. By minimizing the total free energy with respect to ψ_L and ψ_R (Problem 14.15), we can obtain an expression for the Josephson current density J_s, flowing perpendicular to the junction interface from superconductor L to R,

$$J_s = t_{L,R} \chi_L(\mathbf{n}) \chi_R(\mathbf{n}) |\eta_L| |\eta_R| \sin \gamma = J_c \sin \gamma. \tag{14.143}$$

Here, J_c is the critical current density; $\chi_{L,R}$, the basis function, is related to the gap function $\Delta(\mathbf{k})$ through Eq. (14.141); $\Delta_{L,R}(\mathbf{n}) = \eta_{L,R}(\mathbf{n}) \chi_{L,R}(\mathbf{n})$, where $\mathbf{n}$ is the unit vector normal to the junction interface, $\eta_{L,R}(\mathbf{n}) = |\eta_{L,R}| e^{i\phi_{L \cdot R}}$; and γ is defined in Eq. (14.137). $t_{L,R}$ is a constant characteristic of the junction. The basis functions $\chi(\mathbf{n})$ of a Josephson junction electrode with tetragonal symmetry (point group C_{4v}) are listed in Table 14.1. Here, n_x, n_y are the projections of the unit vector $\mathbf{n}$ onto the crystallographic axes $\mathbf{x}$ and $\mathbf{y}$, respectively.

It can be shown from Eq. (14.143), for Josephson junctions between two d-wave superconductors, $\chi(\mathbf{n}) = n_x^2 - n_y^2$, and of which the interface is clean and smooth,

$$J_s = A_s \cos (2\theta_L) \cos (2\theta_R) \sin \gamma, \tag{14.144}$$

Table 14.1 Basis Functions $\chi(\mathbf{n})$ for a Josephson Junction Electrode with Tetragonal Crystal Symmetry

Irreducible	A_{1g}	A_{2g}	B_{1g}	B_{2g}
Representation	s	g	$d_{x^2-y^2}$	d_{xy}
Basis function $\chi(\mathbf{n})$	1	$n_x n_y (n_x^2 - n_y^2)$	$n_x^2 - n_y^2$	$n_x n_y$

where θ_L and θ_R are the angles of the crystallographic axes with respect to the interface, and A_s is a constant characteristic of the junction. However, in real Josephson junctions made with cuprates, the electron wave vector normal to the junction interface can be significantly distorted by interface roughness, oxygen deficiency, strain, and so on. In this limit,

$$J_s = A_s \cos 2(\theta_L + \theta_R) \sin \gamma. \tag{14.145}$$

Flux Quantization of a Superconducting Ring

The flux quantization of a superconducting ring can be written as

$$\Phi_a + I_s L + \frac{\Phi_0}{2\pi} \sum_{ij} \gamma_{ij} = n\Phi_0, \tag{14.146}$$

where Φ_a is due to the flux of an external field, I_s is the supercurrent circulating in the ring

$$I_s = I_c^{ij}(\theta_i, \theta_j) \sin \gamma_{ij}, \tag{14.147}$$

γ_{ij} is defined in Eq. (14.137), and Φ_0 is a flux quantum. It can be shown easily (Problem 14.16) that the ground state of a superconducting ring containing an odd number of sign changes (π ring) has a spontaneous magnetization of a half-magnetic flux quantum, $I_s L \approx (1/2)\Phi_0$, when the external field is zero. Because $I_s = 0$ in the ground state for an even number of π shifts, the magnetic-flux state has an even number of quantization. To summarize,

$$\Phi = n\Phi_0 \quad \text{for } N \text{ even (0 ring)}, \tag{14.148}$$

and

$$\Phi = \left(n + \frac{1}{2}\right)\Phi_0 \quad \text{for } N \text{ odd } (\pi \text{ ring}), \tag{14.149}$$

where N is an integer.

Tricrystal Magnetometry

The multiple-junction ring consists of deliberately oriented cuprate crystals for defining the direction of the pair wave function. The presence or absence of the half-integer flux-quantum effect in such samples as a sample configuration differentiates between various pairing symmetries. In the first tricrystal experiment of Tsuei et al. (Ref. 24), an epitaxial YBCO film (1200 Å thick) was deposited using laser ablation on a tricrystal (100) $SrTiO_3$ substrate. In addition to the three-junction ring located at the tricrystal meeting point, two two-junction rings and one ring with no junction were also made as controls. The design was such that $I_c L \gg \Phi_0$ for observing the half-integer flux quantization. The magnetic flux threading through the superconducting cuprate rings in the tricrystal magnetometry experiments were directly measured by a high-resolution SQUID microscope. A series of tricrystal experiments with various geometrical configurations confirmed that only the $d_{x^2-y^2}$ frustrated configuration showed the half-integer flux-quantum effect.

d-Wave Pairing Symmetry

The evidence from both phase-sensitive symmetry as well as non-phase-sensitive symmetry techniques has conclusively proved that the cuprates have d-wave pairing symmetry. The identification of

d-wave symmetry is based on group theory and the macroscopic quantum coherence phenomena of pair tunneling and flux quantization. However, it does not necessarily specify a mechanism for high-temperature superconductivity.

14.9.5 Search for a Theoretical Mechanism of High T_c Superconductors

The identification of *d*-wave pairing symmetry does not necessarily specify a mechanism for high-temperature superconductors. The solution of this problem should include pairing symmetry, pairing interactions (mediated by phonons, spin fluctuations, or some other bosons) in the presence of strong correlations, and taking into consideration the anomalous normal state and charge segregation and the stripe phase. The observation of a pseudogap in the normal state, with a *d*-wave-like **k** dependence of many underdoped cuprate semiconductors, has generated renewed interest for a suitable theory. Recently, Kresin and Wolf proposed some experiments that will unambiguously resolve the issue.[16]

Anderson noted, "The consensus is that there is absolutely no consensus on the theory of high-T_c superconductivity." Bardeen et al.[2] proposed a microscopic theory of superconductivity in 1957, which was unanimously accepted 46 years after Kammerlingh Onnes discovered superconductivity in Hg in 1911.[15] We do not know how long we have to wait for a satisfactory theory for high T_c superconductivity, which was discovered by Bednroz and Muller in 1986.[3]

PROBLEMS

14.1. Show that Maxwell's equation (neglecting the displacement current **D** as well as replacing **H** with **B** because **j** is the mean microscopic current) can be written as

$$\overrightarrow{\nabla} \times \mathbf{B} = \frac{4\pi}{c}\mathbf{j}. \tag{1}$$

14.2. Minimizing Eq. (14.16) with respect to **A**, show that

$$\overrightarrow{\nabla} \times \mathbf{B} = \frac{4\pi}{c}\mathbf{j}, \tag{1}$$

where

$$\mathbf{j}(\mathbf{r}) = \frac{e^*\hbar}{2im^*}[\Psi^*\overrightarrow{\nabla}\Psi - \Psi\overrightarrow{\nabla}\Psi^*] - \frac{e^{*2}}{m^*c}\mathbf{A}\Psi^*\Psi. \tag{2}$$

14.3. Minimizing Eq. (14.16) with respect to Ψ^*, by first integrating such that all spatial derivatives act on Ψ and then taking functional derivatives with respect to Ψ^*, show that

$$\left[\alpha + \beta|\Psi|^2 + \frac{1}{2m^*}\left(\frac{\hbar}{i}\overrightarrow{\nabla} + \frac{e^*}{c}\mathbf{A}\right)^2\right]\Psi = 0. \tag{1}$$

14.4. Substituting Eq. (14.54) in Eqs. (14.52) and (14.53), we obtained

$$i\hbar\left(\frac{\dot{n}_1}{\sqrt{n_1}} + i\sqrt{n_1}\dot{\phi}_1\right)e^{i\phi_1} = (\varepsilon_1\sqrt{n_1}e^{i\phi_1} + \in\sqrt{n_2}e^{i\phi_2}) \tag{1}$$

and

$$i\hbar \left(\frac{\dot{n}_2}{\sqrt{n_2}} + i\sqrt{n_2}\dot{\phi}_2 \right) e^{i\phi_2} = (\varepsilon_2 \sqrt{n_2} e^{i\phi_2} + \in \sqrt{n_1} e^{i\phi_1}). \tag{2}$$

Show from Eqs. (1) and (2) that

$$\dot{n}_1 = 2\frac{\in n}{\hbar} \sin(\phi_2 - \phi_1) = -\dot{n}_2 = \frac{j}{e^*} \tag{3}$$

and

$$\dot{\phi}_2 - \dot{\phi}_1 = \frac{1}{\hbar}(\varepsilon_1 - \varepsilon_2) = \frac{e^*}{\hbar}(V_2 - V_1), \tag{4}$$

where $n = \sqrt{n_1 n_2}$.

14.5. If we choose $\hat{S}$ such that

$$\hat{H}_1 + [\hat{H}_0, \hat{S}] = 0, \tag{1}$$

in which case, the electron–phonon interaction $\hat{H}_1$ is eliminated apart from a higher-order term. If we choose $\hat{S}$ of the form

$$\hat{S} = \sum_{\mathbf{kq}s'} M_{\mathbf{q}}(\alpha\hat{a}^{\dagger}_{-\mathbf{q}} + \beta\hat{a}_{\mathbf{q}})\hat{c}^{\dagger}_{\mathbf{k}+\mathbf{q},s'}\hat{c}_{\mathbf{k},s'}. \tag{2}$$

From Eqs. (1) and (2), show that

$$\alpha^{-1} = E(\mathbf{k}) - E(\mathbf{k}+\mathbf{q}) - \hbar\omega_{\mathbf{q}} \tag{3}$$

and

$$\beta^{-1} = E(\mathbf{k}) - E(\mathbf{k}+\mathbf{q}) + \hbar\omega_{\mathbf{q}}. \tag{4}$$

14.6. From Eqs. (14.60) and (14.61), the next-order interaction term is $\frac{1}{2}[\hat{H}_1, \hat{S}]$, which is a sum of terms that contain operator products of the form

$$\hat{a}^{\dagger}_{\pm\mathbf{q}}\hat{a}_{\pm\mathbf{q}'}\hat{c}^{\dagger}_{\mathbf{k}'+\mathbf{q}',s'}\hat{c}_{\mathbf{k}',s'}\hat{c}^{\dagger}_{\mathbf{k}+\mathbf{q},s}\hat{c}_{\mathbf{k},s}. \tag{1}$$

Show that because $\mathbf{q}' = -\mathbf{q}$ (from momentum conservation), out of all the combinations, only one does not contain any phonon operators,

$$c^{\dagger}_{\mathbf{k}+\mathbf{q},s}c^{\dagger}_{\mathbf{k}'-\mathbf{q},s'}\hat{c}_{\mathbf{k}',s'}\hat{c}_{\mathbf{k},s}, \tag{2}$$

when

$$\mathbf{k}' \neq \mathbf{k}, \mathbf{k}+\mathbf{q}. \tag{3}$$

14.7. Show from Eqs. (14.60), (14.62), and (14.66) that the proper form of Eq. (2) is

$$H_{eff} = \frac{1}{2} \sum_{\mathbf{k},\mathbf{k}',\mathbf{q},s,s'} |M_{\mathbf{q}}|^2 (\alpha - \beta)\hat{c}^{\dagger}_{\mathbf{k}+\mathbf{q},s}\hat{c}^{\dagger}_{\mathbf{k}'-\mathbf{q},s'}\hat{c}_{\mathbf{k}',s'}\hat{c}_{\mathbf{k},s}. \tag{1}$$

14.8. Substituting the values of α and β from Eqs. (14.63) and (14.64) in Eq. (1) of Problem 14.7, show that

$$<f|H_{eff}|i> = \frac{1}{2} \sum_{\mathbf{k},\mathbf{k'},\mathbf{q},s,s'} <f|V_{\mathbf{kq}}\hat{c}^{\dagger}_{\mathbf{k+q},s}\hat{c}^{\dagger}_{\mathbf{k-q},s'}\hat{c}_{\mathbf{k'}s'}\hat{c}_{\mathbf{k},s}|i>, \tag{1}$$

where

$$V_{\mathbf{kq}} = \frac{2|M_{\mathbf{q}}|^2 \hbar\omega_{\mathbf{q}}}{[E(\mathbf{k}+\mathbf{q}) - E(\mathbf{k})]^2 - (\hbar\omega_{\mathbf{q}})^2}. \tag{2}$$

14.9. Show that if we take the complex conjugate of Eq. (14.79), multiply by $b(\mathbf{k})$, and sum over $\mathbf{k}$, we obtain an equation that agrees with Eq. (14.76), provided $\beta = E$.

14.10. In Eq. (14.83), we derived

$$U \int_{E_F}^{E_F+\hbar\omega_{\mathbf{q}}} \frac{D(x)dx}{2x - E} = 1, \tag{1}$$

where $D(x)$ is the density of states. Show that if we approximate $D(x)$ by $D(E_F)$ in the narrow range of integration, we obtain

$$E = 2E_F - \frac{2\hbar\omega_{\mathbf{q}} \exp[-2/D(E_F)U]}{1 - \exp[-2/D(E_F)U]} \approx 2E_F - 2\hbar\omega_{\mathbf{q}} \exp[-2/D(E_F)U]. \tag{2}$$

14.11. We introduced the $\hat{\alpha}-$ operators in Eq. (14.88):

$$\begin{aligned} \hat{\alpha}_{\mathbf{k}} &= u_{\mathbf{k}}\hat{c}_{\mathbf{k}} - v_{\mathbf{k}}\hat{c}^{\dagger}_{-\mathbf{k}} \\ \hat{\alpha}_{-\mathbf{k}} &= u_{\mathbf{k}}\hat{c}_{-\mathbf{k}} + v_{\mathbf{k}}\hat{c}^{\dagger}_{\mathbf{k}} \\ \hat{\alpha}^{\dagger}_{\mathbf{k}} &= u_{\mathbf{k}}\hat{c}^{\dagger}_{\mathbf{k}} - v_{\mathbf{k}}\hat{c}_{-\mathbf{k}} \\ \alpha^{\dagger}_{-\mathbf{k}} &= u_{\mathbf{k}}c^{\dagger}_{-\mathbf{k}} + v_{\mathbf{k}}\hat{c}_{\mathbf{k}}. \end{aligned} \tag{1}$$

In addition, we use the conditions $u^2_{\mathbf{k}} + v^2_{\mathbf{k}} = 1$, $u_{\mathbf{k}} = u_{-\mathbf{k}}$, and $v_{\mathbf{k}} = v_{-\mathbf{k}}$. Show that these conditions guarantee that the commutation relations for the c-operators also apply to the α-operators.

14.12. From Eqs. (14.91), (14.94), and (14.95), show that

$$\Delta = \frac{U}{2} \sum_{\mathbf{k}} \frac{\Delta}{\sqrt{\varepsilon^2(\mathbf{k}) + \Delta^2}}. \tag{1}$$

14.13. In Eq. (14.102), we obtained

$$E = D(E_F) \int_0^{\hbar\omega_{\mathbf{q}}} \left(\varepsilon - \frac{1}{2}\frac{2\varepsilon^2 + \Delta^2}{\sqrt{\varepsilon^2 + \Delta^2}}\right) d\varepsilon. \tag{1}$$

After integrating Eq. (1), show that

$$E = \frac{D(E_F)}{2}(\hbar\omega_{\mathbf{q}})^2\left[1 - \sqrt{1 + \left(\frac{\Delta}{\hbar\omega_{\mathbf{q}}}\right)^2}\right] \approx -\frac{D(E_F)\Delta^2}{4}. \tag{2}$$

14.14. Because $\Delta(0) \ll \hbar\omega_{\mathbf{q}}$, from Eqs. (14.98) and (14.114), show that

$$\ln\frac{\Delta(T)}{\Delta(0)} = -2\int_0^\infty \frac{dx}{\sqrt{x^2+1}} f\left(\sqrt{x^2+1}\frac{\Delta(T)}{\Delta(0)}\left[\frac{k_BT}{\Delta(0)}\right]^{-1}\right) = F\left(\frac{\Delta(T)}{\Delta(0)}, \frac{k_BT}{\Delta(0)}\right). \tag{1}$$

14.15. The free energy per unit area of Josephson coupling between two superconducting electrodes with order parameters ψ_L and ψ_R (Figure 14.20) can be written as

$$F_j = W\int ds[\psi_L\psi_R^* \exp[i(2\pi/\Phi_0)\int_L^R \mathbf{A}\cdot d\mathbf{l}] + c.c.], \tag{1}$$

where W is a measure of the Josephson coupling strength, and the integral is over the junction interface. By minimizing the total free energy with respect to ψ_L and ψ_R, show that the expression for the Josephson current density J_s, flowing perpendicular to the junction interface from superconductor L to R, is

$$J_s = t_{L,R}\chi_L(\mathbf{n})\chi_R(\mathbf{n})|\eta_L||\eta_R|\sin\gamma = J_c\sin\gamma. \tag{2}$$

Here, J_c is the critical current density; $\chi_{L,R}$, the basis function, is related to the gap function $\Delta(\mathbf{k})$ through Eq. (14.141); $\Delta_{L,R}(\mathbf{n}) = \eta_{L,R}(\mathbf{n})\chi_{L,R}(\mathbf{n})$, where $\mathbf{n}$ is the unit vector normal to the junction interface, $\eta_{L,R}(\mathbf{n}) = |\eta_{L,R}|e^{i\phi_{L,R}}$; and γ is defined in Eq. (14.137). $t_{L,R}$ is a constant characteristic of the junction.

14.16. The flux quantization of a superconducting ring can be written as

$$\Phi_a + I_sL + \frac{\Phi_0}{2\pi}\sum_{ij}\gamma_{ij} = n\Phi_0, \tag{1}$$

where Φ_a is due to the flux of an external field, I_s is the supercurrent circulating in the ring

$$I_s = I_c^{ij}(\theta_i, \theta_j)\sin\gamma_{ij}, \tag{2}$$

where γ_{ij} is defined in Eq. (14.137), and Φ_0 is a flux quantum. Show that the ground state of a superconducting ring containing an odd number of sign changes (π ring) has a spontaneous magnetization of a half-magnetic flux quantum, $I_sL \approx (1/2)\Phi_0$, when the external field is zero. Because $I_s = 0$ in the ground state for an even number of π shifts, the magnetic-flux state has an even number of quantization. To summarize,

$$\Phi = n\Phi_0 \quad \text{for } N \text{ even (0 ring)}, \tag{3}$$

and

$$\Phi = \left(n + \frac{1}{2}\right)\Phi_0 \quad \text{for } N \text{ odd } (\pi \text{ ring}), \tag{4}$$

where N is an integer.

References

1. Aschroft NW, Mermin ND. *Solid state physics*. New York: Brooks/Cole; 1976.
2. Bardeen J, Cooper LN, Schrieffer JR. Theory of Superconductivity. *Phys Rev* 1957;**108**:1175.
3. Bednroz G, Muller KA. Possible high Tc superconductivity in the Ba-Ca-Cu-O system. *Z Physik* 1986; **B64**:189.
4. Bednroz G, Muller KA. Perovskite-type oxides-The new approach to high-Tc superconductivity. *Rev Mod Phys* 1988;**60**:585.
5. Bogoliubov NN. A new method in the theory of superconductivity. *Soviet Phys JETP* 1958;**7**:41.
6. Cohen MH, Falicov LM, and Phillips JC. Superconducting Tunneling.
7. Cooper LN. Bound Electron Pairs in a Degenerate Fermi Gas. *Phys Rev* 1986;**104**:1189.
8. Deaver BS, Fairbank MS. Experimental Evidence for Quantized Flux in Superconducting Cylinders. *Phys Rev Lett* 1961;**7**:43.
9. de Gennes P-G. *Superconductivity of metals and alloys*. Reading, MA: Addison-Wesley; 1992.
10. Ding H, Norman MR, Campuzino JC, Randeria M, Bellmar AF, Yokoya T, et al. Angle-resolved photo-emission spectroscopy study of the superconducting gap anisotropy in Bi2Sr2CaCu2O8+x. *Phys Rev B* 1996;**54**:R9678.
11. Dynes R. McMillan's equation and the Tc of superconductors. *Solid State Commun.* 1972;**10**:615.
12. Doll R, Nabauer M. Experimental Proof of Magnetic Flux Quantization in a Superconducting Ring. *Phys Rev Lett* 1961;**7**:51.
13. Josephson BD. Possible new effects in superconducting tunneling. *Phys Lett* 1962;**1**:251.
14. Josephson BD. The discovery of tunneling supercurrents. *Rev Mod Phys* 1974;**46**:251.
15. Kammerlingh Onnes H. The resistance of platinum at helium temperature. *Comm Phys Lab Univ Leiden* 1911;**119b**:19.
16. Kresin VJ, Wolf SA. Electron-lattice interaction and its impact in high-Tc superconductivity. *Rev Mod Phys* 2009;**81**:481.
17. Landau LD, Ginzburg VL. On the theory of superconductivity. *JETP (USSR)* 1950;**20**:1064.
18. London F, London H. The Electromagnetic Equations of the Superconductor. *Proc. Roy. Soc.* London 1935;**A149**:71.
19. Madelung O. *Introduction to solid state physics*. New York: Springer-Verlag; 1978.
20. Marder MP. *Condensed matter physics*. New York: John Wiley & Sons; 2000.
21. McMillan W. Transition Temperature of Strong-Coupled Superconductors. *Phys Rev* 1968;**167**:331.
22. Meissner W, Ochsenfeld R. A new effect in penetration of superconductors. *Die Naturwissenschaften* 1933;**21**:787.
23. Mercereau. Superconductivity vol. 1, editor. Parks RD. New York: Marcel Dekker; 1961, p. 393.
24. Pals JA, Haeringen W, van Maaren MH. *Phys. Rev. B* 1977;**15**:2592.
25. Stavola M, Krol DM, Schneemeyer LF, Sunshine SA, Fleming RN, Waszczak JV, et al. Raman scattering from single crystals of the 84-K superconductor Bi2.2La0.8Sr2Cu2O8+Δ. *Phys Rev B* 1988;**41**:R5110.
26. Tinkham M. *Introduction to superconductivity*. New York: McGraw-Hill; 1996.
27. Tsuei CS, Kirtley JR. Pairing Symmetry in Cuprate Superconductors. *Rev Mod Phys* 2000;**72**:969.

28. Tsuei CC, Kirtley JR, Chi CC, Yu-Jahnes LS, Gupta A, Shaw T, Sun J-Z, Ketchen MB. Pairing Symmetry and Flux Quantization in a Tricrystal Superconducting Ring of YBa2Cu3O7-Δ. *Phys. Rev. Lett.* 1994;**73**:593.

29. Wu MK, Ashburn JR, Torng CJ, Hor PH, Meng RL, Gao L, et al. Superconductivity at 93 K in a new mixed phase Y-Ba-Cu-O compound system. *Phys Rev Lett* 1987;**58**:908.